small methods
www.small-methods.com

Advances of $LiCoO_2$ in Cathode of Aqueous Lithium-Ion Batteries

Hailing Ma, Fei Wang, Minghai Shen, Yao Tong, Hongxu Wang, and Hanlin Hu**

Aqueous lithium-ion batteries offer promising advantages such as low cost, enhanced safety, high rate capability, and the ability to deliver considerable capacity at 1.8 V, making them ideal candidates for large-scale reserve power sources for renewable energy. However, the practical application of aqueous lithium-ion batteries has been hindered by the poor cycle stability of layered cathode materials, including $LiCoO_2$, in neutral aqueous electrolytes. This review examines the working principles, material limitations, and research progress of aqueous lithium-ion batteries. The types and characteristics of materials used in the cathode of aqueous lithium-ion batteries are summarized, with a primary focus on the attenuation mechanisms of $LiCoO_2$ when used as the cathode material in aqueous electrolytes. Furthermore, this review explores the advancements in utilizing $LiCoO_2$ in the cathode of aqueous lithium-ion batteries, as well as the combination with machine learning. By addressing these critical aspects, this review aims to provide a comprehensive understanding of aqueous lithium-ion batteries and shed light on future development and application prospects.

1. Introduction

After nearly half a century of development, lithium-ion (Li-ion) batteries have become the most advanced electrochemical energy storage technology.[1–3] Compared with lead-acid, nickel-metal hydride, and manganese-zinc dry batteries, lithium-ion batteries exhibit high specific energy density, high power density, and long-term cycle stability, leading to their widespread use in daily life. They have promoted the revolution of portable electronic devices and become the technology of choice for electric vehicles. However, lithium-ion batteries have the following major disadvantages: the battery process conditions are harsh, the abundance of lithium on the earth is low, and cathode materials contain expensive transition metal elements. These factors result in the relatively high cost of producing lithium-ion batteries, and the price is relatively high. In addition, the use of organic electrolytes makes the safety of Li-ion batteries a tricky issue.[4,5] Aqueous lithium-ion batteries have been developed as an extension of lithium-ion batteries, utilizing an aqueous solution of inorganic lithium salts as the electrolyte. This low-cost, high-safety battery technology is of great significance for the utilization of clean and renewable energy.[6–8]

Anode materials have a low cost ratio in lithium-ion batteries. Generally, lithium-ion battery anode materials include carbon-based and non-carbon-based materials.[9,10] Carbon is mainly graphite, graphitized carbon, and amorphous carbon. Non-carbon anode materials are divided into lithium metal nitrides, metal oxides (TiO_2, SnO_2, etc.), silicon-based materials, tin-based materials, new alloys and their composites, and other materials.[11] In terms of potential and capacity, the anode can basically meet the practical application requirements of lithium-ion batteries.[12] The cathode material is not only the limiter of the energy density (capacity, voltage) of the lithium-ion battery, but also the leader of the battery cost. Therefore, it is meaningful to study cathode materials for lithium-ion batteries.

Lithium cobalt oxide ($LiCoO_2$) is one of the most widely used and earliest researched materials in lithium battery cathode materials.[13–15] Due to the temperature difference in the production process, lithium cobalt oxide will form two crystal forms, i.e., layered structure and spinel structure. High-temperature sintering produces a layered structure of lithium cobalt oxide material, while low temperature produces a cubic spinel structure. However, lithium cobalt oxide with a spinel structure is not conducive to the deintercalation of Li ions during the charging and discharging process of lithium batteries. Its electrochemical performance does not meet the application requirements, so it is not used in actual production.[16,17] The layered structure of lithium cobalt oxide has the best electrochemical performance among lithium cobalt oxide materials due to its structure, which is conducive to the transmission of lithium ions, and therefore is the most widely used in lithium batteries. Wang et al.[18] developed a "water-in-salt" electrolyte, which increased the electrochemical window of

H. Ma, F. Wang, Y. Tong, H. Hu
Hoffmann Institute of Advanced Materials
Shenzhen Polytechnic
7098 Liuxian Boulevard, Shenzhen, Guangdong 518055, China
E-mail: yao_tong@szpt.edu.cn; hanlinhu@szpt.edu.cn
H. Ma, H. Wang
School of Engineering and Technology
The University of New South Wales
Canberra, ACT 2600, Australia
M. Shen
School of Energy and Environmental Engineering
University of Science and Technology Beijing
Beijing 100083, China

The ORCID identification number(s) for the author(s) of this article can be found under https://doi.org/10.1002/smtd.202300820

DOI: 10.1002/smtd.202300820

the aqueous lithium-ion battery electrolyte to 3 V. Therefore, the voltage of the aqueous lithium-ion battery is greatly improved, and it also provides more possibilities for the construction of a high-capacity and high-voltage aqueous lithium-ion battery system. The theoretical capacity of $LiCoO_2$ is 274 mAh g^{-1}. But its actual capacity is only 130—140 mAh g^{-1}, which only plays half of the theoretical capacity. This is because the cut-off voltage of the first-generation $LiCoO_2$ is only 4.2 V, so the development of high-voltage $LiCoO_2$ has become the main research direction in recent years.[19,20]

Although layered $LiCoO_2$ is the earliest discovered lithium containing transition metal oxide cathode material, there are still many properties that are not understood. For example, interfacial issues in different systems, properties of heterogeneous polyhedral structures, reasons for high electrocatalytic performance, etc.[21,22] $LiCoO_2$ has the advantages of low production process difficulty, high working voltage, stable discharge current, and long cycle life. However, under high voltage, the increased internal stress of $LiCoO_2$ lattice causes structural collapse and violent interfacial side reactions, leading to irreversible deterioration of battery performance.[23,24] With the strong development of the new energy automobile industry and the electronics industry, the application of lithium-ion batteries is becoming more and more extensive. Higher requirements are put forward for the performance of lithium-ion batteries and aqueous lithium-ion batteries in terms of capacity, cost, cycle performance, voltage, and environmental friendliness. In view of the important role of cathode materials in lithium batteries, the research and development of cathode materials must be further strengthened. As the most widely used cathode material in the electronics market, the development and challenges of $LiCoO_2$ are generally representative. Therefore, $LiCoO_2$ as a research object can still reveal some important scientific questions.

Although $LiCoO_2$ has been studied as a cathode material for lithium-ion batteries for ≈ 40 years, as explained above, there are still many properties that need to be understood urgently. At the same time, $LiCoO_2$ has a serious attenuation problem in aqueous lithium-ion batteries, which remains poorly comprehended with no proposed better solutions. This paper aims to review the problems and challenges associated with $LiCoO_2$ in aqueous lithium-ion batteries, which could provide a reference for other layered materials. The solutions derived from these identified problems hold great significance for enhancing our understanding of the fundamental material properties and facilitating the practical application of materials.

2. Aqueous Lithium-Ion Batteries

2.1. Working Principle of Aqueous Lithium-Ion Batteries

The basic principle of the aqueous battery is the same as that of the non-aqueous battery. When charging, the alkali metal ions flow from the cathode to the anode through electrolyte, and the electrons flow from the cathode to the anode in the external circuit. Since the electrolyte is replaced by an aqueous solution from an organic solution, the prerequisite for the battery reaction to proceed is that lithium ions can be reversibly deintercalated in the aqueous electrolyte. The voltage stability window of the aqueous electrolyte is narrower than that of the organic system. In order to ensure that lithium ions can be reversibly deintercalated in the aqueous solution, it is necessary for the potential of the electrode material to deintercalate lithium to be included in the electrochemically stable potential range of the aqueous electrolyte. Otherwise, if the potential is too high, the electrolyte will generate oxygen; whereas, if the potential is too low, it will generate hydrogen. Therefore, it is very important to choose electrode materials with suitable potential to keep the aqueous electrolyte from decomposing.[25,26]

The electrochemical stability window for pure water is 1.23 V, although kinetic effects can extend the range of stable potentials.[27] For example, in lead-acid batteries[28] and aluminum-oxygen batteries[29] the electrochemical stability windows of the electrolytes used in these two batteries are much larger (>1.23 V) than that of pure water. The pH value of the aqueous electrolyte can affect the stable potential window of the electrolyte, and the specific relationship is shown in **Figure 1a**.[30] When pH = 7-13, the equilibrium voltage value is 3.85-3.50 V (vs Li/Li^+), so it can be seen that most of the cathode materials, such as $LiCoO_2$ and $LiMn_2O_4$, have a higher Li^+ intercalation voltage than 3.9 V (vs Li/Li^+). These relatively high potential materials can exist stably in air and aqueous solution. However, anode materials such as lithium metal, graphite (0–0.3 V vs Li/Li^+), and $Li_4Ti_5O_{12}$ (1-1.5 V vs Li/Li^+) cannot be used for aqueous lithium-ion batteries. In the aqueous lithium-ion battery, once Li^+ is embedded in these materials with relatively low potential, Li in the material will react with O_2, H_2O, etc. to produce LiOH and H_2. It can be seen from Figure 1 that the stronger the acidity of the electrolyte, the higher the oxygen evolution and hydrogen evolution potentials. If the lithium-deintercalation potential of the electrode is 3–4 V (relative to Li/Li^+), it can be used in an aqueous rechargeable lithium-ion battery so that the electrolyte does not evolve oxygen. For example, during the discharge process, lithium ions will be intercalated into the material and reduced (as shown in Figure 1b). Immersing lithium manganese oxide ($LiMn_2O_4$) in 1 M LiOH electrolyte will have the following reaction[31]:

$$Li_{1-x}Mn_2O_4 + xLi^+ + xOH^- \rightarrow LiMn_2O_4 + (x/2)\,H_2O + (x/4)\,O_2 \quad (1)$$

The pH value of the aqueous solution in the equation is 14, and the corresponding anode reaction is as follows[32]:

$$Li_xC_6 + xH_2O \rightarrow C_6 + xLi^+ + xOH^- + (x/2)\,H_2 \quad (2)$$

In addition, Dahn et al.[33] proposed a similar "rocking chair theory" in aqueous systems relative to organic systems, using both organic (1 M $LiPF_6$-EC/DMC(1:1)) and aqueous (1 M Li_2SO_4) reversible systems. Analyzing the experimental results, it is found that the mechanisms of the two systems are parallel in the process of Li^+ deintercalation.

2.2. Advantages of Aqueous Lithium-Ion Batteries

Simply speaking, batteries can be divided into three essential components: cathode, anode and electrolyte. The electrolyte is the transport medium connecting the lithium ions between

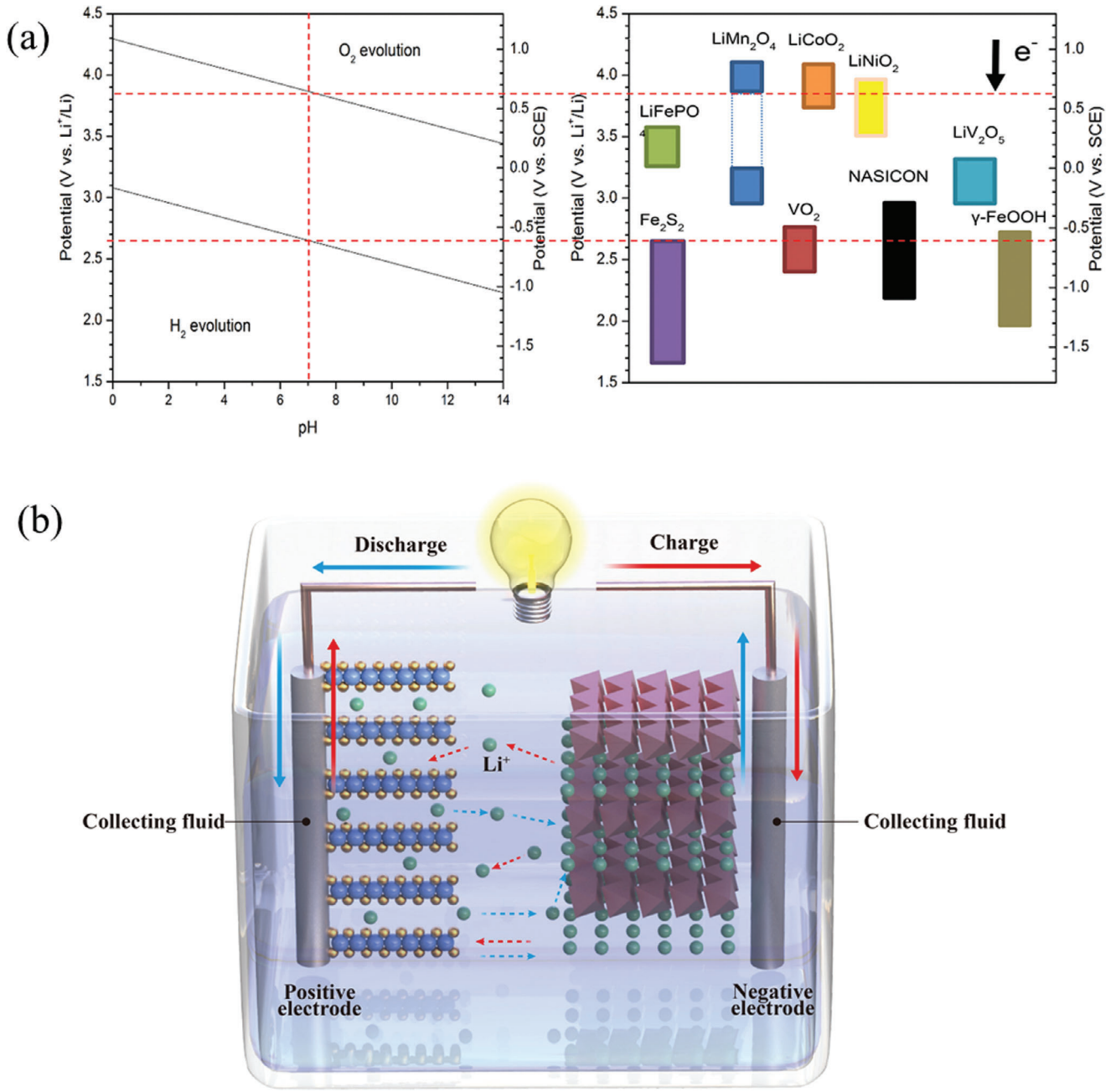

Figure 1. a) The stable potential window of the compound that can reversibly deintercalate lithium in an aqueous solution (compared to lithium electrode and saturated calomel electrode); b) Schematic diagram of the aqueous lithium-ion battery.

the positive and negative phases. The ions in the electrolyte should be able to diffuse rapidly in the system so that the active materials can be fully utilized. While lithium-ion batteries using organic electrolytes offer satisfactory performance, the safety and environmental friendliness of aqueous electrolytes also make them an appealing choice. As production costs decrease and environmental concerns gain more attention, the high conductivity of aqueous electrolytes allows them to exhibit high specific capacity and excellent cycle performance in batteries. Therefore, this section elucidates the advantages of aqueous electrolytes by comparing them with organic electrolytes.

2.2.1. Production Cost

According to data recently released by the global market research organization Markets and Markets, the world battery energy storage system market is expected to reach US$4.4 billion in 2022, and this figure is expected to increase to US$15.1 billion by 2027,

Table 1. Comparison of technical parameters of various types of batteries.[35]

Technology	Electrolyte	Voltage[V]	Costs[€/kWh]
Lead-acid batteries	H_2SO_4 (4–6 M)	2.0	25–40
Nickel-cadmium batteries	KOH (4.7–7 M)	1.2	200–500
Nickel metal hydride batteries	KOH (4.5–7 M)	1.2	275–550
Lithium-ion batteries ($LiFePO_4$)	Lithium salts dissolved in organic solvents	3.4	200-500

with a compound annual growth rate of 27.9%. Lithium-ion batteries account for nearly 20% of the rechargeable battery market due to their high energy density and high power density, and account for 75% of the portable rechargeable battery market. Recently, Jung et al.[34] reported that the worldwide market for renewable energy storage batteries was USD 599 million in 2010 and they predicted it would grow to USD 2.6 billion by 2020.

For new energy vehicles, the batteries used in them currently need to achieve higher energy and power density and longer cycle life, while their production costs should also be minimized.[36] However, the cost of lithium-ion batteries in large-scale applications is still higher than other types of secondary batteries (**Table 1**). While organic electrolytes constitute a substantial cost in producing commercial lithium-ion batteries, it is crucial to clarify that separators, while not negligible, have a comparatively less significant cost contribution. The main cost drivers typically include cathode materials and the manufacturing processes for large-scale production. In addition, during the assembly process of the organic lithium-ion battery, vacuum and no moisture environment is required to isolate the air to prevent the oxidation of the electrolyte, which also increases the production cost of the battery.

Today, practitioners are looking for ways to reduce production costs while maintaining high energy density in batteries. With the advent of aqueous electrolytes, the production cost of lithium-ion batteries will be significantly reduced. The advantages are as follows: (a) $LiNO_3$, LiOH, Li_2SO_4 and other lithium salts are used in the aqueous electrolyte to replace the expensive $LiPF_6$ in the organic electrolyte. (b) The expensive organic separator is replaced by a separator suitable for the aqueous electrolyte. (c) The assembly process no longer requires high standard vacuum and moisture control.

Aqueous lithium-ion batteries utilize water as electrolyte solvent instead of organic solvents, which has several advantages:

1) Security. Compared with organic solvents, water is a relatively safe solvent. Water has a high boiling and flash point, and relatively low flammability and explosiveness, reducing the risk of a battery fire or explosion.
2) Renewability. Water is a renewable and environmentally friendly resource. Utilizing water as an electrolyte can reduce the need for non-renewable organic solvents, helping to reduce environmental impact.
3) Cost-effectiveness. Water is cheaper and more readily available than some organic solvents. This reduces the cost of lithium-ion batteries with water-based electrolytes and facilitates large-scale commercial applications.
4) Electrochemical stability. Water-based electrolytes have good electrochemical stability within a certain range. By optimizing the electrolyte formulation and adding inhibitors, the electrochemical stability of the water-based electrolyte can be improved and the cycle life of the battery can be improved.

However, water-based electrolyte Li-ion batteries also have some challenges and limitations. The redox potential of water is low, which limits the operating voltage of the battery. Dissolved oxygen and water decomposition reactions exist in water, which may lead to battery capacity fading and electrolyte degradation. In addition, aqueous electrolytes can be corrosive to battery materials and require special battery design and management strategies.

In summary, though, utilizing water as an alternative to organic solvents has many potential advantages. However, in-depth research and technical improvements are still needed for practical applications to overcome the challenges associated with water-based electrolytes and improve their performance and reliability.

Reducing the production costs of electrolytes, separators, and battery components for aqueous and non-aqueous Li-ion batteries is key to achieving cost-effectiveness and driving the battery market. Here are some possible approaches:

(a) Electrolyte. In aqueous lithium batteries, water serves as the solvent in the electrolyte solution. In order to reduce production costs, the purity of water quality and treatment costs can be optimized, and the stability and conductivity of electrolytes can be ensured. For non-aqueous Li-ion batteries, reducing the cost of electrolytes can be achieved by optimizing the preparation process, improving the selection of raw materials and synthesis methods. In addition, finding cheaper and sustainable electrolyte substitutes is also a research direction.[37,38]

(b) Separator. Separator is a key component to separate positive and negative electrodes in aqueous and non-aqueous Li-ion batteries. In order to reduce the cost, it is possible to find cheaper separator raw materials, such as polymer materials, and optimize the preparation process to improve the performance and stability of the separator. In addition, new separator materials, such as nanofibrous materials, can be explored to reduce material costs and improve battery performance.[39,40]

(c) Battery pack. In the production of battery components, cost reduction methods include optimizing manufacturing processes and automating production lines to reduce labor and energy costs. In addition, finding cheaper and sustainable

raw materials, such as electrode materials and current collector materials, can also reduce production costs. Standardization and scaling of manufacturing could also help reduce the cost of battery components.[41,42]

(d) Improvement of equipment and technology. Production efficiency can be improved and energy consumption can be reduced by introducing efficient production equipment and technologies, such as automated assembly lines, fine coating technology and thin film deposition technology. The application of emerging technologies, such as 3D printing and flexible electronics, also has the potential to reduce production costs.[43,44]

(e) Circular economy and sustainable development. Adopting the principles of circular economy, such as recycling and reusing used battery components, reducing material waste and using sustainable resources, can reduce production costs and improve resource utilization.[45,46]

It should be noted that reducing production costs often requires a comprehensive approach, including material and process improvement, technology and equipment innovation, and supply chain optimization. At the same time, the balance between cost and performance needs to be weighed to ensure the reliability and safety of the final product and meet market demand.

2.2.2. Safety

The laptop battery recalls in 2006 raised significant consumer concerns regarding battery safety. Instances of battery explosions in mobile phones and hybrid electric vehicles, primarily attributed to heat dissipation issues, have been reported worldwide.[47] Although such explosions are relatively rare, safety issues still limit the large-scale application of lithium-ion batteries to a certain extent, especially in high-power applications.

Reddy et al.[48,49] developed a quality standard for the electrolyte. The standard mainly mentions that the electrolyte should have good conductivity, inertness to active materials, stability at different temperatures, safety during usage, and cheap production costs. Similarly, Aurbach et al.[50] proposed four criteria, which simply are electrochemical window, operating temperature range, safety, and Li-ion battery transport performance. The prominence given to battery safety by both sets of authors is evident, highlighting its critical importance in battery research and development.

Conventional lithium-ion batteries pose a risk of explosion due to short circuits that may occur when the battery undergoes rupture.[51] When a battery ruptures, air can enter its interior, causing the battery to explode. The possible causes of battery safety problems can be summarized in the following four aspects. (1) Overcharging the battery leads to continuous chemical reactions in the fully delithiated cathode material. The unstable structure of the cathode material will generate sufficient heat, which may result in battery rupture and internal explosion. (2) Inadequate heat dissipation will cause the battery to overheat and increase its internal resistance. Overheating will also cause the volatile organic electrolyte to volatilize, thereby increasing the internal pressure of the battery. (3) A short circuit will cause the internal temperature of the battery to rise rapidly, posing a potential danger such as explosion. (4) Improper operation in the production process, etc. may also cause battery rupture or short circuit.

Furthermore, batteries have the potential to explode when operated outside the proper temperature range.[52] For example, when the operating temperature is 90—120 °C, the electrolyte will decompose, and the solid electrolyte interface (SEI) membrane will not be able to protect the carbon anode from side reactions with the electrolyte, which will generate flammable gases inside the battery. When the temperature rises to 130 °C, the separator will melt and the battery will cease functioning, and the cathode material will decompose and release oxygen. Concurrently, the electrolyte is constantly decomposing to produce flammable gases, and when the two gases meet, a violent reaction will occur, resulting in thermal runaway.[53] To address the problem of thermal runaway, researchers have designed a protection circuit as a temperature management system for lithium batteries. The protection circuit can control the battery to work in a safe voltage and temperature range. However, the addition of protection circuits requires additional costs, which conflicts with the original intention of reducing costs.

An alternative approach to addressing the issue of thermal runaway is by utilizing an aqueous electrolyte. The specific heat capacity of water is much larger than that of organic solvents, which allows water to absorb a larger amount of heat. Consequently, the temperature rise in aqueous systems will remain relatively lower compared to organic systems.[54] Moreover, during battery operation, the contact between the water electrolyte and the electrodes will also have a good cooling effect, so no additional heat dissipation system is required for large-scale energy storage.

2.2.3. Conductivity

The good conductivity of the electrolyte is an important guarantee for the battery to exhibit high-rate performance and good reversibility. The conductivity of aqueous electrolyte (10^{-1} Ω^{-1} cm^{-1}) is higher than that of other electrolytes (e.g., organic electrolyte[55] 10^{-3}–10^{-2} Ω^{-1} cm^{-1}, polymer electrolyte[56,57] 10^{-7}–10^{-3} Ω^{-1} cm^{-1}, inorganic solid electrolyte[58] 10^{-7}–10^{-2} Ω^{-1} cm^{-1}). Therefore, the charge-discharge rate of aqueous batteries can be faster than that of organic batteries.[59]

To clarify the fast intercalation kinetics of lithium ions in aqueous electrolytes, the ionic conductivity of $LiNO_3$ solutions as a function of temperature and concentration was compared with organic electrolytes (1 M $LiPF_6$-1:1 EC:DMC).[59] The results showed that the highly concentrated aqueous electrolyte was 17 times more conductive than the organic electrolyte. In addition, researchers found that the lithium-ion transfer activation energy on the surface of the thin film electrode in the water system is lower than that in the organic system, indicating that the deintercalation speed of lithium ions in the water system is faster. This shows that the energy required for the movement of charges in the water system is lower, and the magnification is higher.

2.2.4. Rate Performance

Rate performance refers to the capacity retention rate of a battery as the current density of charge and discharge increases. A higher retention rate indicates better rate performance, while a lower retention rate indicates worse rate performance. When the system has excellent rate performance, more lithium ions can be deintercalated at high charge and discharge current densities. Liu et al.[60] studied the rate performance of olivine-type cathode materials in aqueous and organic systems, respectively, and the results showed that the rate performance of the aqueous system was better. The discharge capacity of $LiMn_{0.05}Ni_{0.05}Fe_{0.9}PO_4/LiTi_2(PO_4)_3$ system in the aqueous electrolyte was measured as 90 and 85 mAh g^{-1} when the current density was 1 and 2 mA cm^{-2}, respectively. In comparison, the discharge capacity in the organic electrolyte dropped to 90 mAh g^{-1} and 70 mAh g^{-1} at the same current densities. This indicates that lithium ions are more easily transported in aqueous electrolytes, even though the aqueous and organic systems have the same concentration of lithium ions. The different rate performance of the two systems is due to the differences in the conductivity of the electrolyte.[61]

Aqueous lithium-ion batteries typically employ a water-based solution, combining water with lithium salts. Aqueous electrolytes exhibit significantly enhanced conductivity surpassing that of many current non-aqueous electrolytes in lithium-ion cells.[62] The conductivity of aqueous electrolyte can reach up to 10^{-1} Ω^{-1} cm^{-1}, higher than organic electrolyte (10^{-3}–10^{-2} Ω^{-1} cm^{-1}), polymer electrolyte (10^{-7}–10^{-3} Ω^{-1} cm^{-1}), and inorganic solid electrolyte (10^{-7}–10^{-2} Ω^{-1} cm^{-1}). Highly concentrated aqueous electrolytes have demonstrated a conductivity that is 17 times greater than organic electrolytes.

The lower viscosity and higher ionic conductivity of aqueous electrolytes compared to non-aqueous electrolytes enable more rapid ion transport,[63] improving the power density and rate capacity of batteries under certain conditions. However, it is crucial to note that despite these advantages, aqueous electrolytes still face limitations at high charging and discharging rates due to the relatively slower diffusion rate and the inherent properties of water molecules, which can restrict ion transport speed and impact power density and rate capacity under these specific conditions.[64]

For non-aqueous lithium-ion batteries, organic solvent-based electrolytes, such as carbonates, ethers, or ionic liquids, are used. Compared with aqueous Li-ion batteries, non-aqueous electrolytes perform better at high rates.[65] In addition, the chemical stability of non-aqueous electrolytes also helps to improve the safety and cycle life of batteries.[66]

Although non-aqueous electrolytes are relatively superior in high-rate performance, they also face some challenges, such as solvent evaporation and battery capacity fading.[7,67] Therefore, there is a certain trade-off in rate performance between aqueous lithium-ion batteries and non-aqueous lithium-ion batteries, and it is necessary to choose the appropriate type according to the needs of specific applications. In practical applications, the rate performance of aqueous and non-aqueous lithium-ion batteries can be further improved by optimizing the electrolyte formulation, improving the electrode material design, and optimizing the battery system.

3. Research Progress of Cathode Materials for Aqueous Lithium-Ion Batteries

The cathode material of the aqueous rechargeable lithium-ion battery must first be able to accommodate the repeated intercalation and deintercalation of lithium ions, so many lithium intercalation compounds used in organic systems can be used in aqueous systems. It should be noted that the lithium-deintercalation potential of the cathode material used in the water system needs to be within the potential range allowed by the electrolyte to ensure that the electrolyte does not undergo oxygen or hydrogen evolution. However, in order to maximize the energy density of the battery, the potential for deintercalating lithium needs to be as high as possible.

Therefore, in summary, some materials can be screened out, such as $LiMn_2O_4$,[68–70] MnO_2,[71–73] $LiCoO_2$,[44,74,75] $LiNi_{1/3}Co_{1/3}Mn_{1/3}O_2$,[76,77] $LiFePO_4$,[78,79] Prussian blue[80,81] and so on. In the early stage, the specific capacity of the material in the water system is low, and the capacity decays rapidly during the cycle. The research suggests that the reasons for the low specific capacity may be: (1) H^+ enters the structure of the material; (2) Li^+ and H^+ exchange during the cycle; (3) water penetrates into the structure; (4) the active substance dissolves in the electrolyte. Researchers have done a lot of modification work on materials.[82–84] Researchers have addressed these issues by modifying cathode materials such as coating and doping and changing the solute concentration of the electrolyte to control the electrode/electrolyte interface.[85,86]

3.1. Phosphate Based Cathode Material $LiFePO_4$

Due to its large free volume, the olivine structure can provide a large space for ion transmission, so it is expected to obtain a cathode material with better performance. $LiFePO_4$ is a typical olivine-structured cathode material for the lithium-ion battery, which was first reported by Goodenough in 1997. The $LiFePO_4$ cathode material belongs to the orthorhombic crystal system (Pnmb space group), and its structure is shown in **Figure 2a**. Li atoms, Fe atoms, and O atoms form LiO_6 and FeO_6 octahedra, respectively, and LiO_6 forms a chain structure in the b-axis direction, so the transport channel of lithium ions has a one-dimensional linear characteristic. The theoretical capacity of $LiFePO_4$ material is 170 mAh g^{-1}, the actual capacity is 140 mAh g^{-1}, the voltage platform is 3.5 V, and the theoretical energy density can reach 550 Wh kg^{-1}. However, compared with other cathode materials, $LiFePO_4$ has a lower lithium-ion diffusion coefficient and relatively lower electrical conductivity due to intrinsic defects. Therefore, the rate performance and kinetic performance of $LiFePO_4$ at room temperature are not ideal. The volumetric energy density cannot reach the theoretical energy density due to the low tap density. To this end, people have tried to improve the electrochemical performance of $LiFePO_4$ by replacing the low-potential Fe^{3+}/Fe^{2+} redox couple with other transition metal ions such as Co, Ni, and Mn.[87,88] There are three main ways to successfully improve the conductivity of materials, which are: (1) surface coating technology,[89,90] such as coating a layer of conductive film on the surface of particles to improve the electronic conductivity of the material, thereby improving the rate

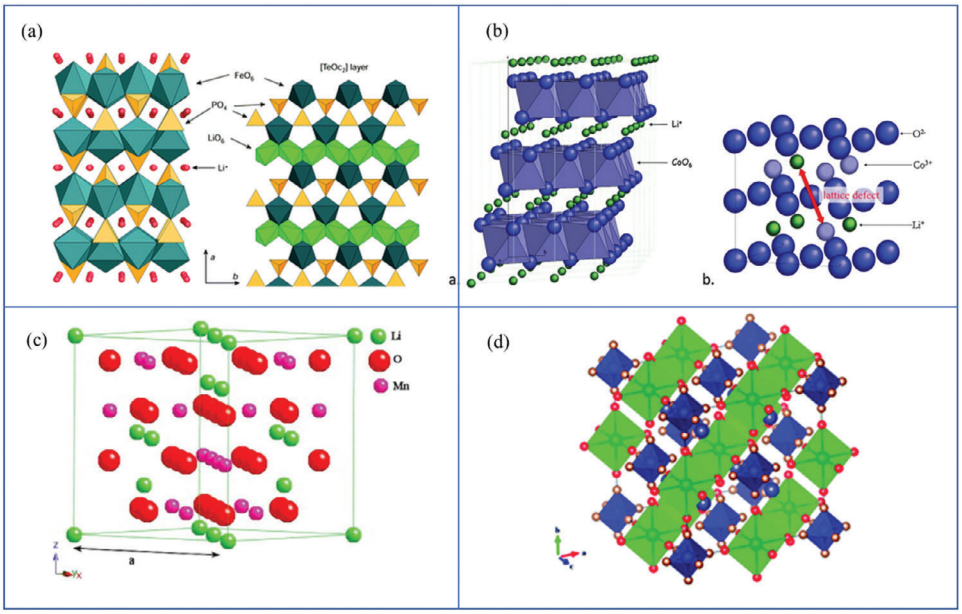

Figure 2. a) Crystal structure of $LiFePO_4$. Reproduced with permission.[96] Copyright 2011, The Royal Society of Chemistry. b) crystal structure of $LiCoO_2$. Reproduced with permission.[97] Copyright 2012, Elsevier Ltd. c) crystal structure of $LiMn_2O_4$. Reproduced with permission.[98] Copyright 2011, Elsevier Ltd. d) crystal structure of Prussian blue. Reproduced with permission.[99] Copyright 2014, The Royal Society of Chemistry.

performance of the material. (2) Regulating the particle size of the material[91] can shorten the diffusion path of lithium ions in the solid phase, and can also reduce point defects and improve the conductivity of lithium ions. (3) Partial replacement of Li sites or Fe sites with cationic doping[92] or substitution and spherification through material morphology, etc.[93] However, the associated costs are higher.

Manickam et al.[94] first proposed the idea of using $LiFePO_4$ as the cathode of an aqueous battery, using zinc foil, a saturated calomel electrode, and a saturated LiOH solution as the counter electrode, reference electrode, and electrolyte, respectively. And the ex-situ analysis of the $LiFePO_4$ deintercalation process was carried out, and the discharge rates of the first cycle, the second cycle, and the fifth cycle were set to 41% (70 mAh g^{-1}), 30% (50 mAh g^{-1}), and 20% (40 mAh g^{-1}), respectively. The delithiation of the electrode during electrochemical oxidation to form $FePO_4$ is similar to that in organic systems, but lithium ions cannot be intercalated well during the reduction process to form a mixture of $LiFePO_4$ and Fe_3O_4. In order to clarify the reason for this phenomenon, He et al.[95] found that 0.5 M Li_2SO_4 (pH = 7) was used as the electrolyte, and found that O_2 and OH^- in the electrolyte would react with the material to generate impurities, which would cause the material performance deterioration dramatically. Then they tried to use the method of coating carbon to isolate the dissolved O_2 and OH^- in the electrolyte and improve the electrochemical performance of the material.

In order to overcome the problems in the application of $LiFePO_4$, researchers focused on three improvement measures. One is to continuously optimize the synthesis process of $LiFePO_4$ to make the particle size of the target product finer (nano-scale) and more uniform. By increasing its specific surface area, the purpose of improving the utilization rate of active materials and reducing the diffusion distance of lithium ions is achieved. The second is to dope metal ions into the LiFePO4 lattice to improve bulk conductivity. The third method involves enhancing the material's surface conductivity by coating with carbon or adding a conductive agent. Commonly used conductive additives mainly include carbon-based materials such as graphite, carbon black, and acetylene black.

3.2. Layered Structure Cathode Material $LiCoO_2$

$LiCoO_2$ was first commercialized as a cathode material for lithium-ion batteries with a layered structure, and it is by far the most widely used cathode material.[100] The $LiCoO_2$ cathode material belongs to the α-$NaFeO_2$ structure (R-3m space group), and its theoretical discharge specific capacity is as high as 272 mAh g^{-1}, while the actual discharge specific capacity is only 140 mAh g^{-1}.[101] Its ionic and electronic conductivity are relatively high, and it is easy to synthesize, and its charge and discharge platform is ≈4.0 V. Figure 2b is a schematic diagram of the structure of the $LiCoO_2$ cathode material. Li^+ and Co^{3+} are respectively located in alternating octahedral positions in the cubic close-packed oxygen layer, with two-dimensional lithium-ion insertion and extraction channels. The O atoms are distorted cubic close-packed, and the Co^{3+} layer and Li^+ layer are located on both sides of the oxygen layer, occupying the octahedral void position.[102] During the charge and discharge process, lithium ions can shuttle back and forth between the layers to perform reversible intercalation and deintercalation reactions. Because lithium ions reciprocate between the strongly bonded CoO_2 layers, the conductivity of lithium ions in the layered material $LiCoO_2$ is high, and the diffusion coefficient is large, ≈10^{-7}–10^{-9} cm^2 s^{-1}.

At the same time, the edge-sharing octahedral CoO_6 interacts in the form of Co-O-Co, so the electronic conductivity is also high. Therefore, $LiCoO_2$, a lithium-ion cathode material with a layered structure, has high ionic and electronic conductivity.[103,104] As the most widely used material in organic systems,[105] $LiCoO_2$ was also used to explore its performance in aqueous systems. In the work of Wang et al.,[106] they tested the Cyclic Voltammetry(CV) of $LiCoO_2$ in two systems and found that the materials showed three pairs of distinct redox peaks in both systems through CV comparison. In the water system, a saturated calomel electrode was used as a reference electrode, and a platinum electrode was used as a counter electrode. The peak voltages of the two main reduction peaks of the material were 0.71 and 0.87 V, respectively. This is consistent with the value of the lithium-deintercalation voltage in the organic system. And in the CV curve of the aqueous system, the delithiation peak of $LiCoO_2$ material can be observed, indicating that the delithiation occurs before the oxygen evolution reaction.

It can be seen from the above that the electrochemical mechanism of materials is similar in aqueous and organic systems. However, early researchers reported that when the electrolyte is LiOH solution, the H+ intercalation material will be preferential to the Li^+ intercalation in the LiOH electrolyte, and later it was found that using $LiNO_3$ or Li_2SO_4 as the electrolyte can realize the reversible Li^+ in the material. Ruffo et al.[59] studied the electrochemical performance of the material in 0.1, 1.0, and 5.0 M $LiNO_3$ solutions, respectively. After testing the CV, it was found that the reduction reaction occurred around 0.9 V (the standard hydrogen electrode was used as the reference electrode). And as the concentration of the electrolyte increases, the potential of the reduction reaction also increases linearly. It shows that the reversible lithium ion deintercalation is more than the hydrogen ion deintercalation. Tang et al.[106] prepared a nano-$LiCoO_2$ for use as cathode material for aqueous Li-ion batteries. This material has a charge-discharge specific capacity of 143 mAh g^{-1} at a high current of 1000 mA g^{-1}. When the current density increases to 5000 mA g^{-1} and 10 000 mA g^{-1}, the discharge specific capacity can still maintain 135 and 133 mAh g^{-1}, respectively. The excellent rate performance of the material can be attributed to the small particle size of the material itself and the excellent electrical conductivity of the aqueous electrolyte.

In order to solve the existing problems of $LiCoO_2$, the researchers adopted methods such as surface coating and bulk phase doping to inhibit the undesirable phase transformation to a certain extent. It has significant effects in preventing structure collapse and enhancing the reversibility of material crystal structure. However, due to the scarcity of cobalt resources, the price has been rising continuously in recent years, resulting in the rising cost of lithium-cobalt cathode materials, so it has no advantage in price.

3.3. Other Cathode Materials

So far, a wide range of cathode materials for lithium-ion batteries have attracted attention in research and application. These include MnO_2, which has been studied for its unique properties, along with more conventional materials such as $LiNi_{1/3}Co_{1/3}Mn_{1/3}O_2$ and Prussian blue analogues, among others MnO_2 has α-, β-, γ-, δ-, ϵ-, λ- and other crystal forms.[107,108] These crystalline forms of MnO_2 have been used in supercapacitors.[109,110] Among these crystal forms, the γ-, δ-, and λ-types have the ability to accommodate lithium ion intercalation, so they are tried to be used in aqueous lithium-ion batteries. Deutsher et al.[111] explored the electrochemical performance of λ-MnO_2, using LiCl as the electrolyte, the discharge capacity of the material in the first cycle is 160 mAh g^{-1}, and the lithium-ion can be repeatedly deintercalated in subsequent cycles, but the material's capacity fades quickly, and after 60 cycles, only 50 mAh g^{-1} is left in the discharge specific capacity. Yuan et al.[112] investigated the electrochemical performance of γ-MnO_2. γ-MnO_2 can achieve reversible lithium deintercalation in LiOH solution. After assembling the material with the activated carbon anode into a full battery, the discharge specific capacity in the first cycle is 35 mAh g^{-1}, and it maintains 78% after 1500 cycles. Qu et al.[113] found that δ-MnO_2 also behaved like γ-MnO_2. The CV test found that the material had obvious redox peaks, but did not provide a specific charge-discharge capacity.[114]

$LiMn_2O_4$ is the earliest material used as the cathode of ALIBs, with a theoretical specific capacity of 148 mAh g^{-1}. It is a spinel-structured hexagonal crystal (space group Fd3m) with three-dimensional lithium-ion channels, as shown in Figure 2c. The 32e tetrahedral site is $O2^-$, the Mn3+/4+ occupies the 16d octahedral site, and the Li^+ occupies the 8a tetrahedral site. During the charge and discharge process, Li^+ is reversibly extracted and inserted from the $LiMn_2O_4$ lattice. Tian et al.[115] prepared nanoscale spinel $LiMn_2O_4$ by solid phase grinding at room temperature, and tested its electrochemical behavior in $LiNO_3$ solutions with different concentrations. The results showed that with the increase of $LiNO_3$ concentration, the reaction potential shifted obviously. And the current intensity of the two pairs of redox peaks is the largest in 5 M $LiNO_3$ solution, indicating better reversibility of the electrode reaction.

The use of $LiMn_2O_4$ as the cathode material for aqueous lithium-ion batteries has some significant advantages. First, it has good stability, and the manganese element is non-toxic and basically has no pollution to the environment.[61,116] The second is low cost. The price of manganese is lower than that of nickel. The use of lithium manganese cathode material can greatly reduce the cost of batteries. The third is high specific capacity. The theoretical value of the specific capacity of lithium-manganese materials can reach 148 mAh g^{-1}, while the actual value is as high as 160–190mAh g_{-1}. Fourth, the lithium-manganese cathode material is a spinel-type material with a three-dimensional tunnel structure.[61] This structure is very beneficial to the intercalation and extraction of Li^+, which is better than the cathode material with layered structure.

However, the main problems in the application of $LiMn_2O_4$ as the cathode material of lithium-ion batteries are: ①The electrode material will undergo disproportionation reaction in the electrolyte, and then be gradually dissolved. ② Jahn-Teller distortion will occur during the deep discharge process, resulting in a change in the volume of the spinel lattice, resulting in the loss of electrode components. ③ When charging at high voltage, the electrolyte may become unstable. The existence of the above-mentioned problems makes the capacity of lithium-manganese materials gradually decay during use. To overcome the occurrence of the above-mentioned phenomena,

modification treatment must be carried out. At present, the commonly used modification treatment methods are mainly doping and surface treatment, and the doped metals mainly include lithium, germanium, titanium, lead, iron, cobalt, nickel and so on.[117]

The ternary material $LiNi_{1/3}Co_{1/3}Mn_{1/3}O_2$ is a promising substitute material for $LiCoO_2$ in non-aqueous systems, so it is also used by researchers to study its properties in aqueous systems. Wang et al.[118] explored the effect of different pH values of the electrolyte on the material properties, and the results showed that the pH value of the electrolyte would affect the stability of the material. When pH = 13, the peak potential of the CV curve of the material remains unchanged, indicating that the stability of the material is the best when pH = 13. However, when pH = 13, the oxygen evolution reaction in the electrolyte will cover the reduction peak of the material, so the material cannot completely deintercalate lithium when pH = 13. And under the condition of low pH value, the H^+ in the electrolyte will intercalate into the material and cause side reactions.

Prussian blue has the original hexacyanometallic framework structure, and its chemical formula can be written as $AxPR(CN)_6$. Among them, nitrogen-coordinated transition metal cations (P) and hexacyanometallic complexes ($R(CN)_6$) form a face-centered cubic structure with large interstitial A sites, as shown in Figure 2d. Wessells et al.[119] were the first to propose Prussian blue as the cathode material for aqueous batteries. They used the co-precipitation method to prepare two electrode materials: copper hexacyanoferrate (CuHCF) and nickel hexacyanoferrate (NiHCF). The two materials can perform intercalation and deintercalation of various ions, such as Li^+, Na^+, K^+, NH^{4+}. The electrochemical performance of the material was tested in $LiNO_3$ solution at pH = 2. The results show that the discharge capacity of the material at a rate of 41.7C can maintain 60% of that at a rate of 0.83C, but the cycle performance of the material is poor because the Prussian blue active material will dissolve in the electrolyte during the cycle. In the next section, this paper will elaborate on the development history, research progress, application system and existing problems of $LiCoO_2$.

4. Attenuation Mechanism of Lithium Cobalt Oxide Cathode Material

4.1. Phase Transition Mechanism and Decay Mechanism of O3 Phase $LiCoO_2$

The space group of layered $LiCoO_2$ is R-3m. Li^+ and Co^{3+} layers are arranged alternately in the octahedral position formed by the cubic close-packed $O2^-$. LiO6 and CoO_6 octahedra stack with each other, sharing edges. The arrangement order of the O layer is ABCABC, so it belongs to the O3 phase.[120] Due to the large difference in charge and ion size between Li^+ and Co^{3+}, Co interacts more strongly with O. Li^+ can conduct 2D diffusion in the interlayer of CoO_2, and its diffusion coefficient is 10^{-11}–10^{-12} m2 s^{-1}.[121] The Li^+ diffusion path obtained by DFT simulation is that Li^+ escapes from the octahedral position, first passes through a transition position of an adjacent tetrahedron, and then reaches the adjacent octahedral position. This diffusion mode has the lowest energy barrier.[122] When $LiCoO_2$ undergoes electrochemical deintercalation of Li^+, the phase transition mechanism is that when charging starts, $LiCoO_2$ undergoes an insulator/metal phase transition (the original $LiCoO_2$ shows insulator properties due to the presence of only low-spin state Co^{3+}:$3d^6$($t_{2g}^6e_g^0$); after being charged and oxidized, $Co^{3+/4+}$:t_{2g}^{6-x} with holes is obtained and has metallic properties).[123,124] Upon charging ≈4.2 V, the hexagonal O3 phase transforms into a Li^+ ordered monoclinic (space group C2/m) phase transition.[125,126] Continuing to remove Li^+ beyond 0.5 will continue to return to the O3 phase. When the voltage reaches 4.5 V, the O3 phase transforms into the H1-3 phase ($R\bar{3}m$ space group, six CoO_2 layers as a unit cell). Complete de-Li^+ will give O1 phase (a single CoO_2 layer is a unit cell).[127–129]

The O3 phase $LiCoO_2$ is not only superior to the aforementioned spinel oxide cathode and lithium iron phosphate cathode in terms of Li^+ diffusion, but also has a very high volumetric energy density with a theoretical capacity of 274 mAh g^{-1}. For example, when charged to 4.4 V, it has a specific capacity of 170 mAh g^{-1} and a volumetric energy density of 2820.3 Wh L^{-1}, which is comparable to the current high-nickel ternary material 811. Therefore, the researchers' research on high-pressure $LiCoO_2$ is very numerous. With various theoretical studies, coating and doping modification, the voltage of $LiCoO_2$ has gradually increased. However, there is no clear time node for its research progress. According to the actual product launch time of high-voltage lithium cobalt oxide, it has mainly gone through three generations of products:

1) 1991, ≈140 mAh g^{-1}, $Li_{1-x}CoO_2$, x≈0.5, ≈4.25 V versus Li/Li^+. It was initially found that the cycle performance of $LiCoO_2$ decreased when the voltage was higher than 4.25 V. At the same time, it was found that at 4.2 V, that is, when 0.5 Li was removed, there would be a transition from the hexagonal phase to the monoclinic phase. The researchers linked the performance decay to this phase transition and studied it carefully. The reason for the performance decay at this stage is summarized as that the hexagonal/monoclinic phase transition is not fully reversible and will cause a huge volume change. And the surface and interface side reactions are serious, such as the dissolution of Co.[130,131]
2) 2013, ≈155 mAh g^{-1}, $Li_{1-x}CoO_2$, x≈0.57, ~4.35 V versus Li/Li^+. After more than ten years of research, it is found that the hexagonal/monoclinic phase transition at 4.2 V is not the main factor affecting the performance.[132–134] People have gradually increased the voltage of $LiCoO_2$ by means of doping and coating.[135,136]
3) 2014, ≈170 mAh g^{-1}, $Li_{1-x}CoO_2$, x≈0.64, ≈4.4 V versus Li/Li^+. With the deepening of understanding and unremitting exploration of $LiCoO_2$, it is found that under high voltage (below 4.5 V), surface side reactions, Co dissolution and other issues are the main reasons that affect the performance of $LiCoO_2$ materials. Therefore, more efficient modification methods for $LiCoO_2$ have been developed.[137–139]

The order-disorder phase transition occurring in the 4.2 V region impairs the diffusion of Li+ ions. Additionally, lattice expansion along the c-axis and slippage along the ab direction result in mechanical strain on the particles. In fact, the phase transition is highly reversible, and the size fluctuation of $LiCoO_2$ here is only 0.2–0.3%, with limited impact on the

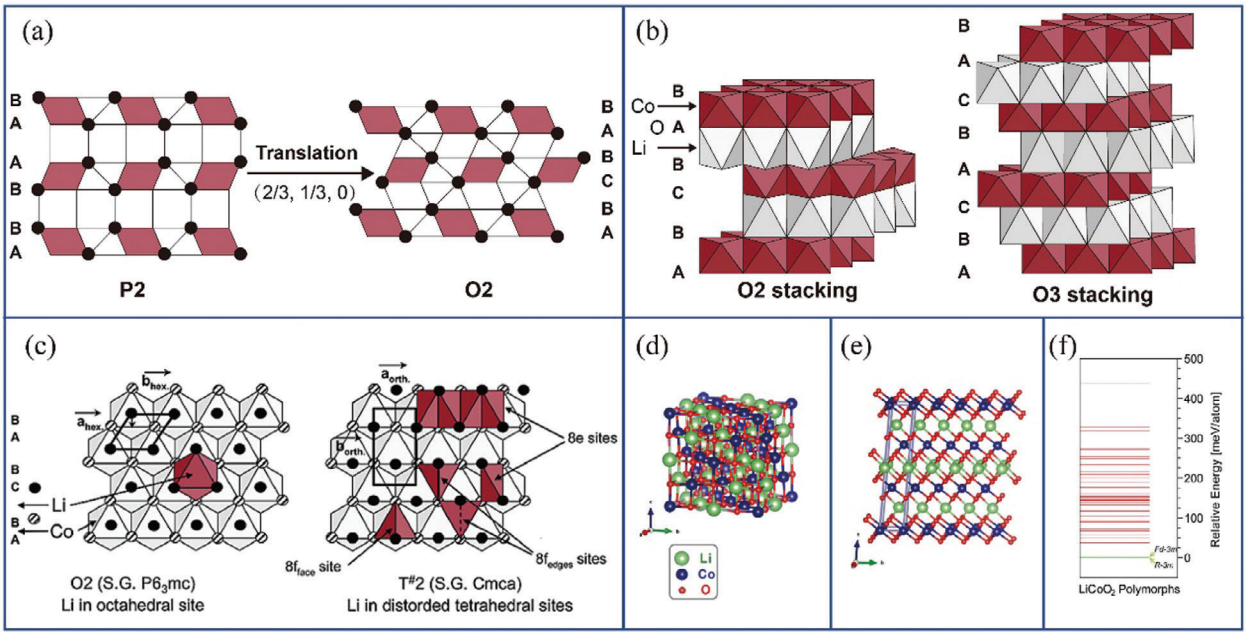

Figure 3. a) Schematic diagram of the structural transition from P2 to O2 observed in the ion exchange process from the [110] direction, black dots represent oxygen ions. Reproduced with permission.[152] Copyright 2001, Elsevier Ltd. b) Schematic diagram of the crystal structure of $LiCoO_2$ in O2 and O3 phases; c) Observing the structure of O2 and T#2 from the [001] direction, the black solid circles represent the O atoms above the Li layer. Reproduced with permission.[153] Copyright 2004, American Chemical Society. d) Crystal structure of $LiCoO_2$ in spinel phase; e) $LiCoO_2$ in O3 phase; f) The relative energy scale of $LiCoO_2$ with two different structures. Reproduced with permission.[154] Copyright 2018, American Chemical Society.

performance.[140] When charged to 4.5 V and above, the capacity fading mechanism of $LiCoO_2$ in organic electrolyte is more complicated, which is not only related to the crystal structure and electronic structure of the material itself, but also to the type of electrolyte and the properties of the interface.[141] The O3-H1-3-O1 phase transition started at 4.5 V, the slip phase transition reversibility of the CoO_2 lamella was reduced, and the particles underwent a c-axis shrinkage greater than 3%. Since the energy band of $Co^{3+/4+}$:3d overlaps with the top of the energy band of $O2^-$:2p, when $LiCoO_2$ is charged to a higher potential, $O2^-$ will provide charge compensation and oxidation reaction will occur. O_2 will be released from the lattice, causing damage to the material.[142] In addition, some researchers have found that when charged to a higher potential, the interface of $LiCoO_2$ is unstable, and a spinel phase with low electrochemical activity will be formed.[143,144] In addition, some researchers believe that some solvents in the organic electrolyte will react with the surface of $LiCoO_2$, causing the $LiCoO_2$ interface to change or even dissolve.[145,146] Nowadays, the technical difficulties faced by people to further increase the voltage of O3 phase $LiCoO_2$ are more severe. Fortunately, there are also recent studies on high-voltage $LiCoO_2$ (≈200 mAh g^{-1}, $Li_{1-x}CoO_2$, x≈0.67, 4.5–4.6 V vs Li/Li^+) at 4.5 V and above.[147–151] This is due to the deepening of the understanding of materials, and the researchers' design of doped element types and surface modification is more directional.

4.2. Structure and Phase Transition Mechanism of O2 Phase $LiCoO_2$

Delmas et al. performed ion exchange on $Na_{0.7}CoO_{1.96}$ of P2 phase (heating in LiCl methanol solution at low temperature) to obtain $Li_{0.93}CoO_{1.96}$ of O2 phase.[104] Due to the strong oxidation of Co^{4+} in lithium layered oxides, the P2 phase $Na_{0.7}CoO_{1.96}$ is driven to undergo ion exchange and reduction reactions in solution. Finally, the O2 phase $Li_{0.93}CoO_{1.96}$ with a lower Co valence state is obtained. Based on X-ray diffraction (XRD) analysis, it is preliminarily inferred that Li^+ ions occupy octahedral sites, characterized by specific unit cell parameters (a = 2.806±0.004 Å, c = 9.52±0.01 Å) and belonging to the space group (P3m1), indicating a distinct crystallographic arrangement that influences the electrochemical properties. This ion exchange reaction can only be carried out at low temperature, and if the temperature is higher or the O2 phase $LiCoO_2$ is heated, the O2 phase will transform into the O3 phase. Therefore, the researchers believe that the O2 phase $LiCoO_2$ is a thermodynamic metastable state. The researchers also found that the P2 or O2 structure did not transform to the spinel $LiCoO_2$ structure even when ion exchange was performed at relatively high temperatures. Carlier et al. used magnetic tests, 7Li MAS NMR and neutron diffraction to prove that stoichiometric O2 phase $LiCoO_2$ was obtained. It was found that Li+ and Co^{3+} in the coplanar CoO_6 and LiO_6 octahedra are offset from their octahedral centers due to electrostatic repulsion. The specific atomic positions, unit cell parameters (a = 2.80247(4) Å, c = 9.5358(3) Å) and space groups (P63mc) of O2 phase $LiCoO_2$ were obtained. The mechanism of this ion exchange reaction was elaborated in detail, as shown in **Figure 3a**.[152] During the transition from P2 to O2, one of the two CoO_2 lamellae slipped (2/3, 1/3, 0). Na^+ breaks out from the original triangular prism sites, and the newly formed octahedral sites are occupied by Li^+. Along the [001] direction, the stacking pattern of the O layer changes from ABBAAB of P2 to ABCBAB of O2. Figure 3b shows the difference in the structure of $LiCoO_2$ in O2

and O3 phases. In the O3 phase $LiCoO_2$, the LiO_6 octahedron and the CoO_6 octahedron share the upper and lower sides, and three layers of CoO_2 are required to form a unit cell. In the O2 phase $LiCoO_2$, one side of the LiO_6 octahedron is co-edge with CoO_6, and the other side is co-planar with the CoO_6 octahedron. Two layers of CoO_2 are required to form a unit cell.

Mendiboure et al. first studied the structural changes of O2 phase $LiCoO_2$ during electrochemical delithiation and chemical delithiation.[155] Dahn et al. used in situ XRD to study the structural change of O2-phase $LiCoO_2$ electrochemically delithiated.[156] They all found that a new phase appeared when the lithium content was 0.5-0.7, and returned to the O2 phase at higher potentials. Carlier, Horn, Delmas, Ceder, etc. systematically studied the phase transition of O2 phase $LiCoO_2$ during delithiation, and found that T#2 phase appeared when the lithium content was 0.52-0.72. At higher potentials the O6 phase appears, continues charging and returns to the O2 phase.[157,158] As shown in Figure 3c, during the transition from O2 phase to T#2 phase, one of the two CoO2 lamellas slipped (1/3, 1/6, 0). Since the position of O in this phase does not occupy the classical A, B, or C position, the # symbol is added to distinguish the T2 phase.[153]

The T#2 phase belongs to the orthorhombic crystal system and the Cmca space group. At this time, three twisted tetrahedral sites are generated for Li^+ to occupy, as shown in Figure 3c, they are 8e site, 8fedge site, and 8fface site. Through neutron diffraction, theoretical calculation, electron diffraction and other means, the researchers concluded that in the T#2 phase, Li^+ mainly occupies the lower-energy 8e tetrahedral position. While the 8f sites are less stable compared to the 8e sites, they nonetheless accommodate a minor proportion of Li^+ ions. The researchers predict that there are some stable ordered phases during charge and discharge, such as the Li^+ ordered structure T#2′ phase at a Li content of 0.5. The researchers proved by spin polarization calculations that the ordered structure O6 phase produced when Li content is ≈0.3 may not be due to the reduction of Li content or the different distribution of Co^{3+}/Co^{4+} in the two CoO_2 slabs. From the calculated formation energy, the formation energy of O6 phase is the lowest when the Li content is 0.3.

The discovery and research of O2 phase $LiCoO_2$ provides new possibilities for high-performance layered oxide cathode materials. For example, the O2-phase $Li_{2/3}Ni_{1/3}Mn_{2/3}O_2$ layered material discovered by Paulsen and Dahn et al. can provide a reversible specific capacity close to 200 mAh g^{-1} in Li-ion batteries.[159] At the same time, they also confirmed that although O2-phase $LiCoO_2$ is metastable compared to O3-phase $LiCoO_2$, the transformation from O2 to O3 will occur at high temperature, but the electrochemical performance of O2-phase $LiCoO_2$ is comparable to that of O3-phase $LiCoO_2$.[156] In the O2-phase lithium-rich material with a single-layer Li_2MnO_3 superstructure synthesized by Xia et al. by ion exchange, it can provide a specific capacity of ≈400 mAh g^{-1}. And the electrochemical reversibility of the material has been greatly improved compared with the Li-rich materials in the O3 phase.[160] So far, there are relatively few reports on O2 phase layered materials. Although researchers have conducted more detailed studies on materials in terms of crystal structure, theoretical calculations, and phase transition mechanisms, there are still many speculative conclusions and unsolved scientific problems. Therefore, O2 phase layered materials still have many important properties, waiting to be discovered by many researchers.

4.3. Structure and Phase Transition Mechanism of Spinel Phase $LiCoO_2$

Low-temperature LT-$LiCoO_2$ synthesized at 400°C was first reported by Gummow et al.[161] According to XRD analysis, the LT-$LiCoO_2$ has a similar structure to the layered O3 phase $LiCoO_2$. However, the lattice constant of LT-$LiCoO_2$ is c/a = 4.9, compared with the layered O3 phase $LiCoO_2$ (c/a = 4.99), the O atoms in its lattice have ideal cubic close packing. Through neutron diffraction refinement, it is believed that there is a mixed phenomenon of Li and Co in LT-$LiCoO_2$, that is, 6% of Co occupies the 3a position of Li, while the excess Li occupies the 3b position of Co. Such a structure not only makes the unit cell parameter c/a = 4.9, but also the value of c/a is maintained with the Li^+ intercalation and deintercalation during the charge and discharge process, so the Co occupying the octahedral position of the Li layer plays a role in stabilizing the structure. Rossen et al.[162] assigned LT-$LiCoO_2$ to the Fd-3m space group of the spinel structure. In the lattice, O occupies the 32e site, Li and Co occupy the 16c and 16d octahedral sites, respectively, with slight shuffling. It has been found that it is difficult to synthesize pure phase $LiCoO_2$ in the spinel phase. Therefore, the mixing of Co and Li is relatively small. Electrochemical tests found that the main voltage plateau of LT-$LiCoO_2$ was 3.3–3.9 V, with obvious voltage hysteresis, which was also significantly lower than the 3.8–4.3 V of O3-phase $LiCoO_2$. The difference in electrochemical behavior is due to the spinel structure of LT-$LiCoO_2$. The structure of materials under different sintering conditions was studied by Yang Shao-Horn et al. It is believed that the spinel $LiCoO_2$ is synthesized at 400 °C as the main phase, and when the sintering time or temperature is prolonged, the spinel phase will transform into a layered O3 phase $LiCoO_2$. Therefore, the structure of LT-$LiCoO_2$ is between the ideal layered structure $(Li)_{3a}[Co]_{3b}O_2$ and the ideal spinel structure $(Li_2)_{16c}[Co_2]_{16d}O_4$. Among them, 75% Co and 25% Li alternately stacked with 25% Co and 75% Li cation layers. The presence of Co at the 16c octahedral sites may affect the diffusion of Li^+ at the interstitial sites in the $[Co_2]O_4$ spinel framework. Hence lower voltage and higher voltage hysteresis. Kim et al. used first-principles calculations to analyze the phase transition mechanism of spinel phase $LiCoO_2$ during the electrochemical deintercalation of Li^+.[154] As shown in Figure 3d–f, they first calculated that the energy of the layered O3 phase $LiCoO_2$ and the spinel phase $LiCoO_2$ are close. However, the O3 phase $LiCoO_2$ is a ground state structure at all temperatures, so the spinel phase $LiCoO_2$ can easily transform to the O3 phase $LiCoO_2$. Due to the slow kinetics, the spinel phase $LiCoO_2$ can exist stably at lower temperatures. Through the ex-situ XRD test and the migration energy barrier calculation of Li^+, it is believed that Li^+ is released from the tetrahedral position of $LiCoO_2$ in the spinel phase, and preferentially enters the vacant octahedral position when embedded, as shown in **Figure** 4a. The voltage hysteresis occurs due to the difference in the migration energy barrier of Li^+ diffusion during charging and discharging, as shown in Figure 4b. This theoretical calculation result can help researchers understand the complex electrochemical process of spinite $LiCoO_2$. Since the O3

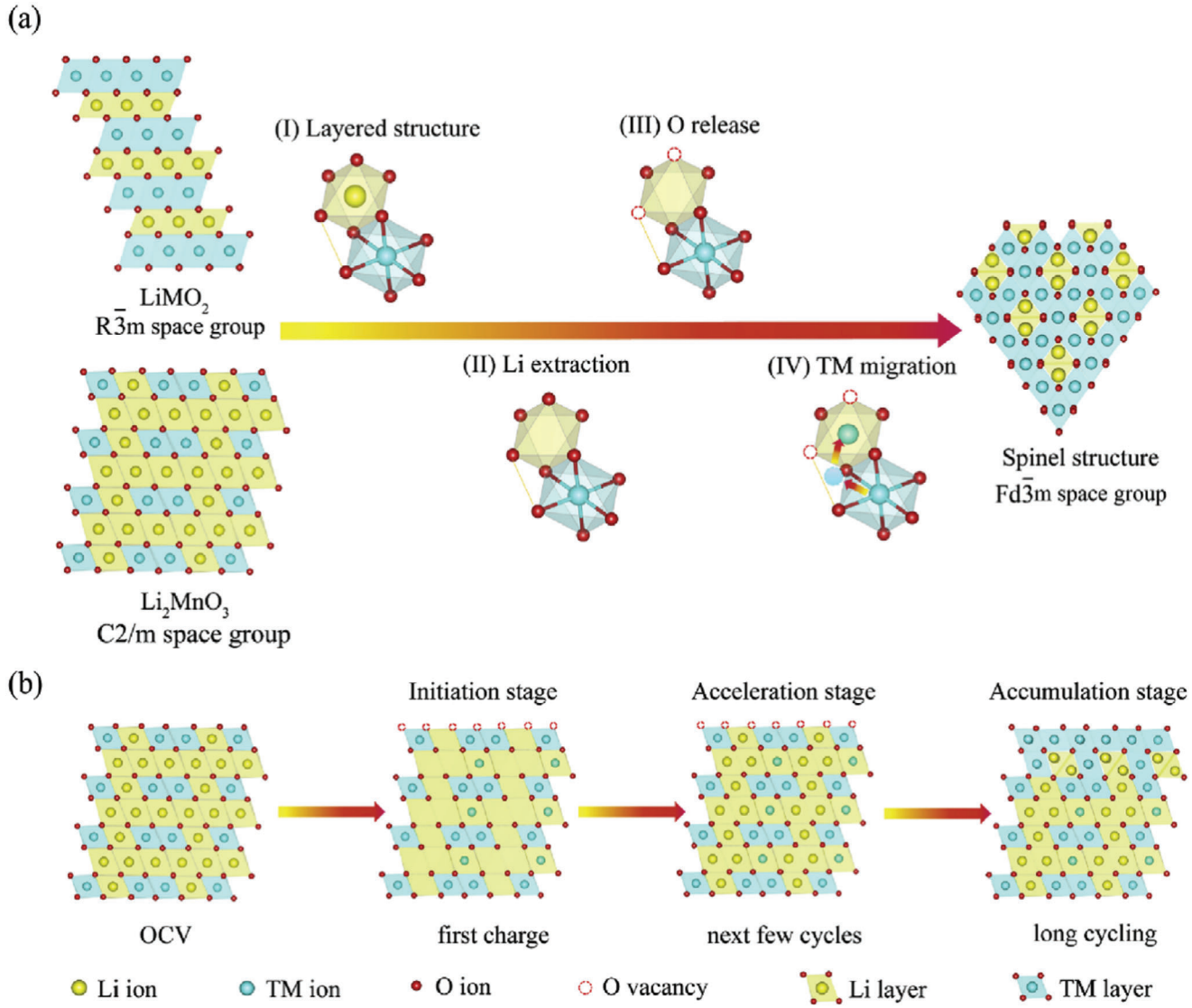

Figure 4. Schematic diagram of the structure and phase transition mechanism of lithium-rich cathode materials from layered phase transition to spinel phase a) and during electrochemical cycling b).[163] Copyright 2019, Elsevier Ltd.

phase $LiCoO_2$ with layered structure changes from layered to spinel at the interface or even in the bulk phase during the electrochemical cycle, the discovery and research of the spinel phase $LiCoO_2$ is very important.[163]

In summary, the unstable surface chemistry is the main reason for the capacity fading when the charge cut-off voltage exceeds 4.2 V but not higher than 4.5 V. The poor structural stability is the main reason for the rapid capacity decay when the charge cut-off voltage exceeds 4.5 V. But it must be pointed out that when the charging cut-off voltage exceeds 4.2 V, oxygen loss,[20] cobalt dissolution,[164] side reactions of electrolyte[165] and irreversible phase transition[166] of the surface are also factors that cannot be ignored. In order to solve the above problems, researchers have proposed a variety of solutions, such as element doping,[140] surface coating,[125] co-modification of doping and coating,[167] etc., to prolong the cycle life of LiCoO2 under high cut-off voltage. Typical doping elements include Mg, Al, Ti, Ni, Zr, Mn, and Sb, etc. In addition to single-element doping, it also includes dual-element and multi-element co-doping.[168,169]

5. Application of $LiCoO_2$ in Cathode of Aqueous Lithium-Ion Battery

The potential of O3 phase $LiCoO_2$ to deintercalate Li^+ is above 3.7 V (vs Li/Li^+), which can exist stably in aqueous electrolyte. Considering the electrochemical window of aqueous electrolytes, the voltage range for practical applications in aqueous electrolytes (such as 1 M Li_2SO_4 pH≈7 solution) is 0–1.1 V (vs SCE). A reference electrode is an electrode used to establish a reference base for electrochemical measurements. In electrochemical experiments, commonly used reference electrodes are standard hydrogen electrode (SHE) and saturated calomel electrode (SCE). The difference between the potential of these electrodes and the

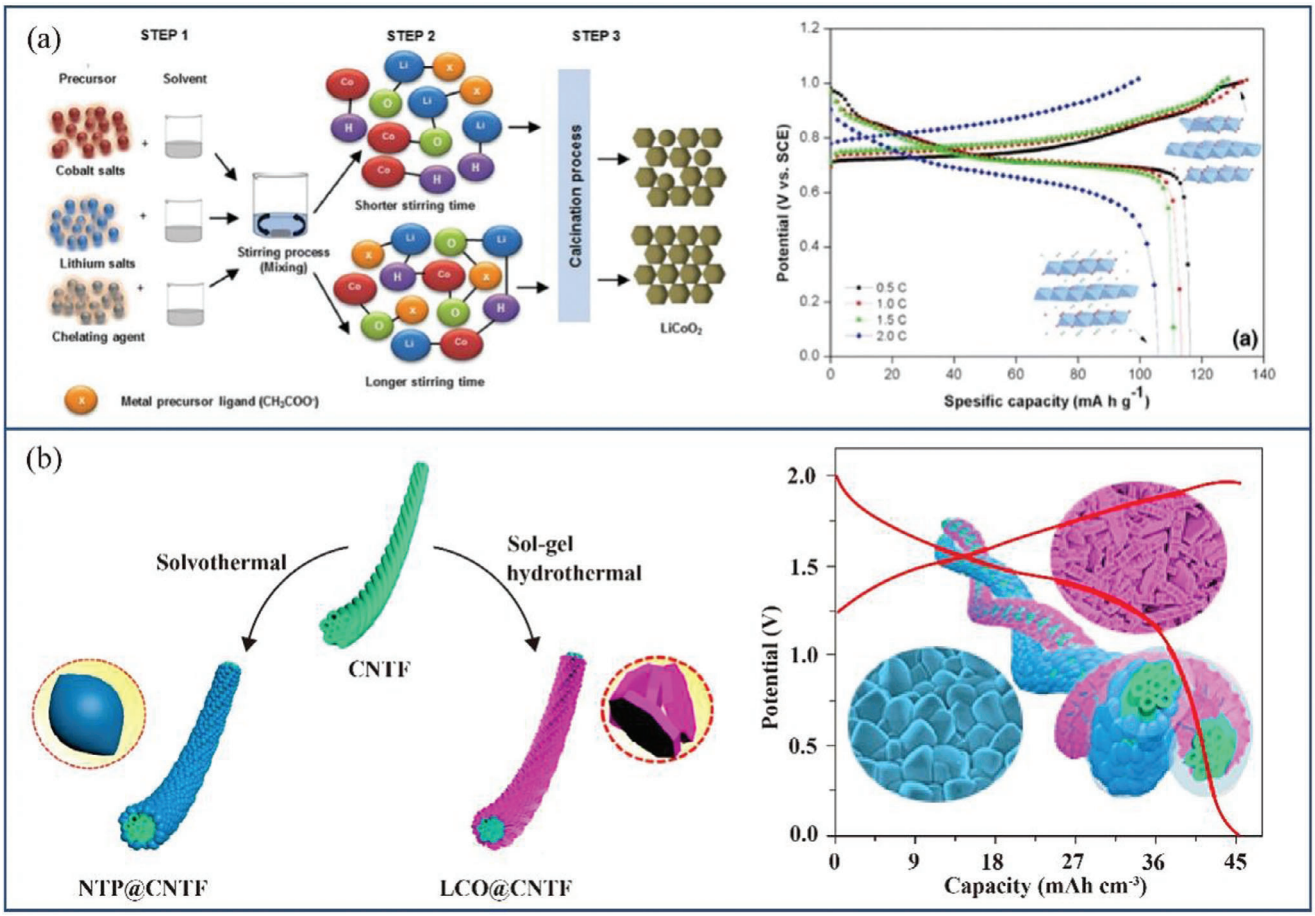

Figure 5. a) Synthetic pathway and specific capacity of hexagonal $LiCoO_2$. Reproduced with permission.[170] Copyright Springer-Verlag GmbH Germany 2017 b) synthesis strategy and specific capacity of LCO@CNTF. Reproduced with permission.[172] Copyright 2020, American Chemical Society.

potential of the reference electrode can be expressed by the following formula:

$$E_{SHE} = E_{SCE} + E^{0}_{SCE} \quad (3)$$

$$E_{SHE} = E_{Li/Li+} + E_{Li/Li+0} \quad (4)$$

In the formula, E_{SHE} is the measured value converted to the potential compared to the standard hydrogen electrode. E_{SCE} is the actual potential measured using the SCE reference electrode. E_{SCE0} is the standard electrode potential of the SCE compared to the standard hydrogen electrode.

This formula describes how the electromotive force of a battery is determined by the potential difference between the reference electrode and the other electrodes. The potential of the reference electrode is measured and determined by an international standard, so it can be used as a reference base to measure the potential of other electrodes.

$E_{Li/Li+}$ is the electrode potential relative to Li/Li^+. $E_{Li/Li+0}$ is the standard electrode potential of Li/Li^+ relative to the standard hydrogen electrode. It is known that $E_{SCE0} = 0.2415$ V and $E_{Li/Li+0} = -3.045$ V, then:

$$E_{Li/Li+} = E_{SCE} + 3.2865 \ \text{V} \quad (5)$$

Equation (5) can convert the E_{SCE} measured in the aqueous three-electrode system into $E_{Li/Li+}$. Therefore, for 0–1.1 V (vs SCE) in practical applications, this voltage range can be obtained relative to the voltage range of 3.2865–4.3865 V (vs Li/Li^+) in organic systems with Li metal as the anode. Theoretically, $LiCoO_2$ can exert a capacity close to 150 mAh g^{-1} in an aqueous lithium-ion battery, which is already a very impressive capacity.

Aziz et al.[170] synthesized $LiCoO_2$ samples at different stirring times. The hexagonal $LiCoO_2$ stirred for 30 h produced the highest peak intensity and the smallest particle size. Studies have shown that its particle size is 0.32–0.47 µm, and $LiCoO_2$ shows a high initial specific capacity of 115.49 mAh g^{-1} (as shown in **Figure 5**a). Liu et al.[171] used metal cadmium as the anode and nanometer $LiCoO_2$ as the cathode, and formed a battery in 0.5 M Li_2SO_4 and 10 mM $Cd(Ac)_2$ neutral aqueous solution. Studies have shown that the battery has an energy density of 72 Wh kg^{-1}, its electrochemical performance is comparable to that of nickel-cadmium batteries, and its environmental performance is better. With the increasing demand for power supply of portable electronic devices, flexible and wearable energy storage devices with low cost and high safety are urgently needed. Man et al.[172] synthesized a binder-free $LiCoO_2$ polygonal sheet-like cathode material (LCO@CNTF) and a football-shaped $NaTi_2(PO_4)_3$ anode material (NTP@CNTF) on carbon nanotube fibers, respectively,

as shown in Figure 5b. A quasi-solid fibrous flexible aqueous rechargeable lithium-ion battery (FARLIB) was assembled in a saturated Li_2SO_4 solution. The study shows that the LCO@CNTF electrode has excellent capacity and extraordinary rate performance in saturated Li_2SO_4 solution. At the same time, due to the synergistic effect of LCO@CNTF and NTP@CNTF, the capacity of FARLIB is 45.24 mAh cm^{-3}, and the energy density is 67.86 mWh cm^{-3}, which is better than most reported FARLIB. The battery also has good flexibility and can retain 94.74% capacity after bending 3000 times, which provides new prospects for the design of wearable energy storage devices.

Although $LiCoO_2$ can exhibit high specific capacity in aqueous lithium-ion batteries, the reported use of $LiCoO_2$ as the cathode material of aqueous lithium-ion batteries (with electrolyte pH ≈ 7) has been limited by its poor cycling stability and potential safety concerns due to the instability of cobalt-based materials in aqueous environments. Usually only the cycle performance of charging and discharging at high rates is shown, and the number of cycles is small[25,106,173] Some reports have shown that the attenuation of $LiCoO_2$ in neutral electrolytes with pH ≈ 7 is very serious in charge-discharge cycles[174] Much work has been done to improve the cycle stability of aqueous Li-ion batteries.[175–177] Among them, the pH value of the neutral electrolyte is increased, and it is found that the increase of the pH value can significantly improve the cycle stability of layered materials such as $LiCoO_2$, $LiCo_{1/3}Ni_{1/3}Mn_{1/3}O_2$, etc. It is found that $LiCo_{1/3}Ni_{1/}3Mn_{1/3}O_2$ is stable in neutral solution during charging. However, H^+ will participate in the intercalation reaction near 0.3 V (vs SCE) during discharge, and it is difficult for the protons embedded in the material to come out reversibly. And it will hinder the diffusion of Li^+ in the material, resulting in increased electrode polarization[178] By increasing the pH value, the intercalation potential of the proton can be shifted in the negative direction. This shift enhances the electrochemical stability of $LiCo_{1/3}Ni_{1/3}Mn_{1/3}O_2$ when used in aqueous electrolytes.

Although the H^+ in the neutral aqueous electrolyte would cause attenuation of the layered material due to intercalation, the 1 M Li_2SO_4 aqueous electrolyte at low pH would lead to a more severe attenuation of $LiCoO_2$. In a neutral solution with pH ≈ 7, $[H^+] \approx 10^{-7}$ M, the research object is a button battery. If it is considered that the mass of $LiCoO_2$ in the cathode is 10 mg, and the content of the electrolyte is 0.1 mL (slightly excessive), then in this battery, $[LiCoO_2] = 1.02\times10^{-4}$ mol, $[H^+] = 1\times10^{-11}$ mol. Therefore, trace protons only cause partial attenuation of $LiCoO_2$. And during the cycle, H^+ may also be consumed by hydrogen evolution reaction.

As we all know, there are a lot of proton-containing substances in the air, which will be adsorbed on the surface of the material, and excessive heat treatment of the material will also lead to the loss of protons. Therefore, trace protons embedded in materials are very difficult to characterize.[179,180] At the same time, the high stability of spinel-structured cathode materials in neutral aqueous electrolytes does not seem to be affected by trace protons. Wang et al.[181] reported the use of film-forming additives to improve the cycling stability of $LiCoO_2$ in aqueous batteries, as shown in **Figure 6a**. They found that surface Co dissolution and surface remodeling of $LiCoO_2$ occurred at high potentials. However, this phenomenon is also common in organic electrolytes, and they use water-in-salt electrolytes, which are quite different from traditional 1 M Li_2SO_4 low-concentration electrolytes. G. Charles Dismukes et al.[182] found that $LiCoO_2$ undergoes surface reconstruction in both alkaline and neutral electrolytes, as shown in Figure 6b. It can be seen that the trace H^+ intercalation in the neutral electrolyte is only part of the reason for the attenuation of $LiCoO_2$ cathode materials in aqueous lithium-ion batteries. On the other hand, it is still necessary to further study the properties of the electrode-electrolyte interface, such as the bonding of H^+ on the surface of $LiCoO_2$, the dissociation of adsorbed H_2O, the migration and dissolution of Co elements, and the irreversible phase transition mechanism of the surface interface, etc.

Ruffo et al.[25] studied the electrochemical performance of $LiCoO_2$ at different $LiNO_3$ concentrations. The results showed that the rated voltage increased with increasing electrolyte concentration, which indicated that Li^+ was reversibly intercalated and deintercalated, not H^+. In the voltage window of 0.55-1.15 V (vs SHE), $LiCoO_2$ has little polarization effect and can be stably maintained for more than 90 cycles. In the voltage window of 0.55–1.2 V (vs SHE), the specific capacity reaches approximately 115 mAh g^{-1} (**Figure 7a**). In addition, the Coulombic efficiency of $LiCoO_2$ obviously decreases with the increase of junction-stop voltage. Tang et al.[106] used a solution-gel method to synthesize nano-$LiCoO_2$. Nano-$LiCoO_2$ can discharge 143 mAh g^{-1} at a current density of 1000 mA g^{-1}. The discharge specific capacities are 135 and 133 mAh g^{-1} at current densities of 5000 and 10 000 mA g^{-1}, respectively. This excellent rate performance and cycling stability are attributed to the nanoscale of the material and the fast diffusion of ions in the aqueous electrolyte (Figure 7b).

Poor overcharge resistance is another challenge for lithium cobalt oxide materials as cathodes for aqueous lithium-ion batteries. When layered $LiCoO_2$ is charged to 4.2 V versus Li/Li^+, half of the Li^+ is released from the interlayer, and the continued removal of Li^+ will lead to a change in the spatial law between Li^+ and Li^+ vacancies, and the repulsion between the cobalt layers increases, and the crystal along the c-axis direction expands, $LiCoO_2$ transforms from the hexagonal phase to the monoclinic phase, and the layered structure is unstable. Therefore, in practical applications, the actual capacity of $LiCoO_2$ is often only half of the theoretical capacity.

In response to this problem, surface coating with metal oxides to suppress the generation of oxygen vacancies in the surface layer, and a well-designed surface structure to suppress the phase transition process from the initial stage are effective methods to solve the problem of voltage decay. The reason for the improved electrochemical performance can be attributed to the fact that the surface coating reduces the contact between the electrode and the electrolyte and reduces the occurrence of side reactions. The expanded layer space caused by lattice expansion after coating broadens the transport channel of lithium ions. It is beneficial to the intercalation/deintercalation of lithium ions during charge and discharge.

Optimizing design and improving manufacturing process efficiency can accelerate the discovery of $LiCoO_2$ cathodes and help gain a deeper understanding of material properties and mechanisms. Through the application of machine learning, the development and improvement of $LiCoO_2$ cathodes materials can be accelerated to promote the development of lithium-ion battery technology.

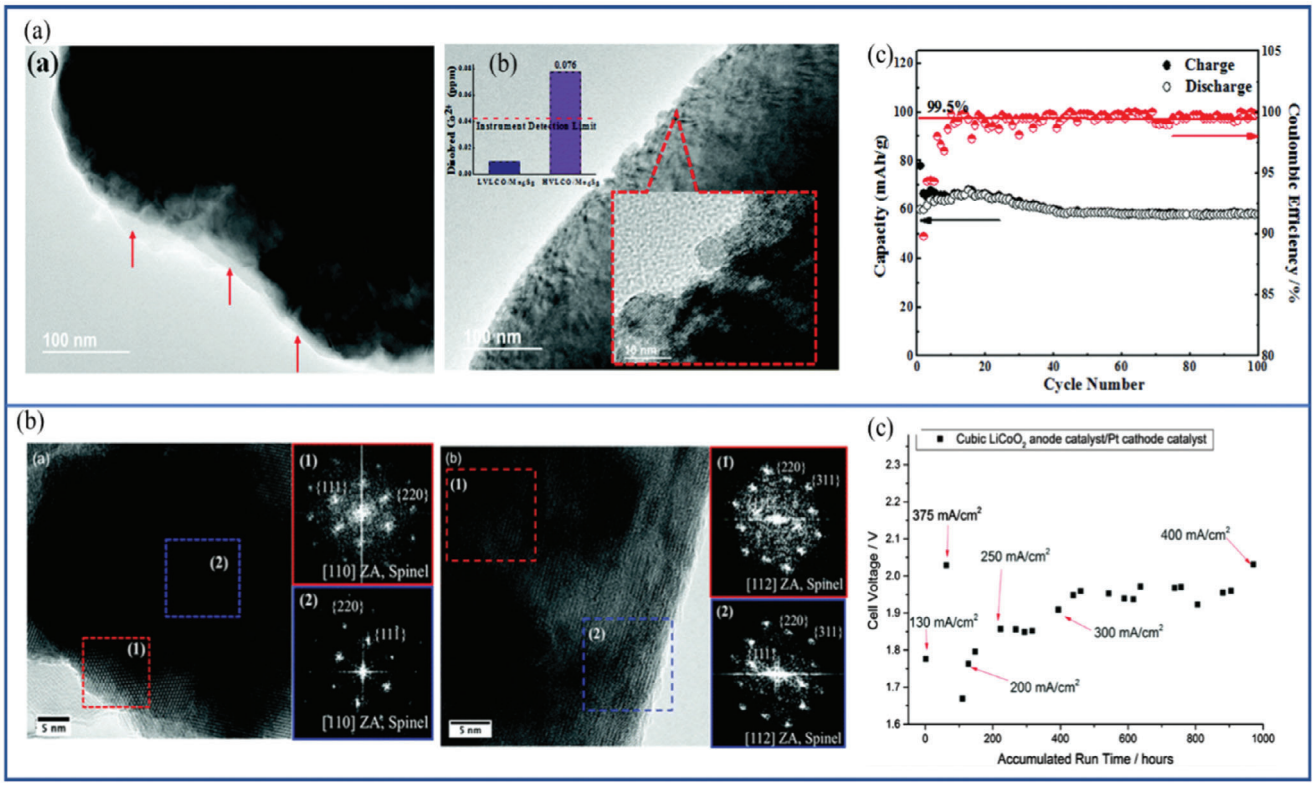

Figure 6. a) Co dissolution, surface remodeling and cycle stability of $LiCoO_2$ surface at high potential. Reproduced with permission.[181] Copyright 2016, The Royal Society of Chemistry. b) surface remodeling and cycle stability of $LiCoO_2$ in alkaline and neutral electrolytes. Reproduced with permission.[182] Copyright 2016, The Royal Society of Chemistry.

6. Application of Machine Learning Method in $LiCoO_2$ Cathode

6.1. Development of Machine Learning Models

The basic workflow of machine learning includes data input, model learning and final output. The data input stage includes data collection and preprocessing, while the model learning stage is to identify and analyze the data or explore the implicit relationship between the data through a certain algorithm. The final output stage is to use the optimized model to predict or analyze unknown data. Machine learning can be divided into three categories: supervised learning, unsupervised learning, and reinforcement learning. Supervised learning learns from labeled inputs and outputs, unsupervised learning finds patterns in unlabeled data, and reinforcement learning uses rewards and punishments to improve a program's decision-making.

In machine learning, choosing the right algorithm is very important. Common machine learning algorithms include Naive Bayes,[183] K-Nearest Neighbor,[184] Support Vector Machine,[185] Decision Tree,[186] Random Forest,[187] Maximum Expectation Algorithm,[188] Artificial Neural Network[189] and Deep Learning, etc. Each algorithm has its characteristics and scope of application, and choosing an appropriate algorithm can improve the accuracy of the machine learning model.

In short, machine learning is a discipline that studies how to make machines think and learn like humans.[190] It enables computers to learn autonomously and make intelligent decisions through a large amount of data and algorithmic rules, and is widely used in tasks such as classification, regression, clustering, and dimensionality reduction. Choosing the right algorithm and optimizing the model can improve the effectiveness and accuracy of machine learning.

6.2. Enhancing Aqueous Lithium-Ion Batteries through Machine Learning-Aided Optimization of Cathode Material $LiCoO_2$

In recent years, materials science research has developed rapidly, generating a large amount of data information.[191,192] Machine learning algorithms can mine effective information from these data, especially for large-scale, high-dimensional data sets generated by computing, which can identify feature patterns and extract hidden rules and correlations. Machine learning techniques are mainly used in four aspects in materials science research: guiding the synthesis and development of new materials, fitting spatial energy and force fields, optimizing theoretical potential functions of materials, and combining with high-throughput computing.[193,194] Among them, machine learning technology can replace traditional experimental methods in the synthesis and development of new materials and improve work efficiency.[195,196] For example, in the research on the synthesis of halides, machine learning technology can solve tedious chemical synthesis problems and improve the accuracy

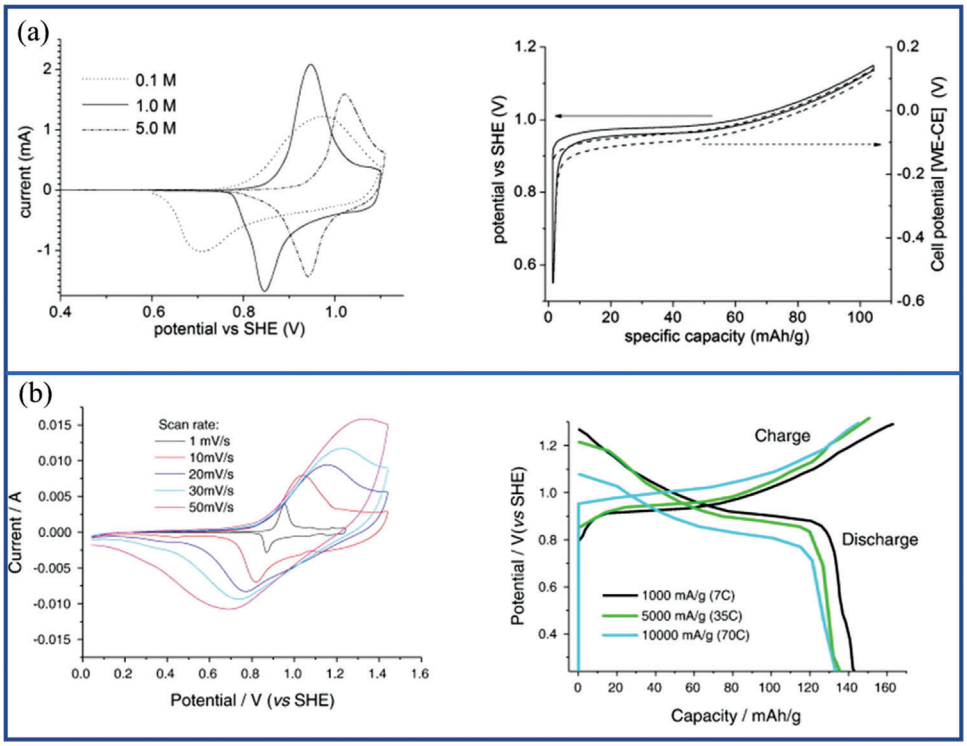

Figure 7. a) CV and charge-discharge performance of $LiCoO_2$ at different $LiNO_3$ concentrations. Reproduced with permission.[25] Copyright 2009, Elsevier Ltd. b) CV and charge-discharge performance of nano-$LiCoO_2$ at different current rates. Reproduced with permission.[106] Copyright 2010, Elsevier Ltd.

of halide structure determination. In addition, machine learning technology can also be used in the design and development of molecular structures of new materials through methods such as reinforcement learning.

At present, the design and development of materials mainly rely on traditional trial-and-error experimental methods, which are inefficient and costly.[197] Applying machine learning to material design and development can extract the implicit relationship between parameters from a large amount of experimental data, find performance influencing factors and changing rules, establish predictive models, and guide the design of new materials. In the development of specific functional materials, it is very important to find the correspondence between structure and performance. When existing theories cannot explain the relationship between structure and properties, using machine learning for training, learning and predicting the structure and properties of materials is a feasible method.[198] For example, in the application of $LiCoO_2$, a cathode material for water-based lithium-ion batteries, machine learning models can predict the structure and properties of materials and mine their corresponding relationships. This approach can improve the efficiency and accuracy of materials design and provide guidance for the synthesis and development of new materials.

Li et al.[199] proposed a machine learning method called atomic table convolutional neural network, which can predict the formation energy, band gap, and superconducting transition temperature Tc of compounds by continuously learning suitable features during training. The accuracy of the model exceeds the results of standard DFT calculations. Through data augmentation techniques, the model can not only accurately predict the superconducting transition temperature of superconductors, but also distinguish superconductors from non-superconductors. Using this model, potential materials with high superconducting transition temperatures can be screened out, which can provide guidance and inspiration for the design and development of higher-performance cathode materials for aqueous lithium-ion batteries.

The atomic table convolutional neural network approach provides a new machine learning approach for predicting the properties and behavior of compounds. It is applied to lithium cobalt oxide, a cathode material for aqueous lithium-ion batteries, and can provide important guidance and inspiration for the design and development of materials. The microstructure of a material has a direct impact on its macroscopic properties. Therefore, the characterization and regulation of the microstructure is crucial to the theoretical basis of materials and the design and development of new materials.[200] Traditional materials characterization methods rely on experimental equipment and researchers' experience, which is time-consuming and error-prone. On the other hand, machine learning techniques provide new ways to study the microstructure of materials. For example, the monolayer structure of chemically precipitated phases can be modeled using machine learning simulation methods. The mapping relationship between microstructure and macroscopic properties can be established with convolutional neural network. The background of the measured spectra can be identified and removed using unsupervised probabilistic learning methods. These methods not only improve the accuracy

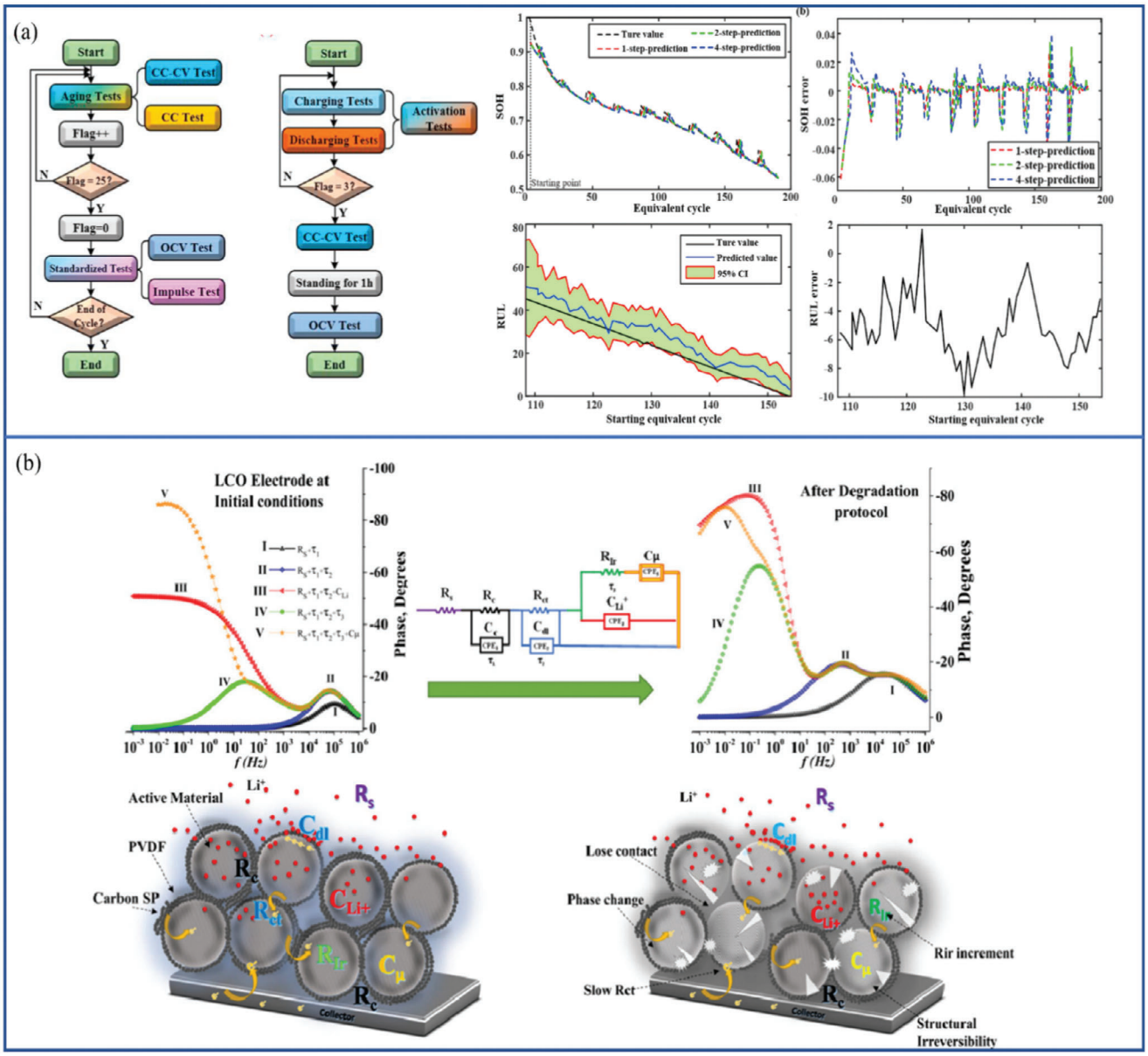

Figure 8. a) Short-term state of health and remaining useful life prediction method based on particle filter algorithm for $LiCoO_2$ batteries. Reproduced with permission .[201] Copyright 2021, Elsevier Ltd. b) EIS reconstruction based graphical method to detect electrode modification effects. Reproduced with permission[202] Copyright 2021, Elsevier Ltd.

of characterization, but also reduce the dependence on manual manipulation.

Deep learning techniques can be applied to the characterization of microstructures in 3D samples. By combining unsupervised machine learning techniques, topological classification, and image processing methods, Subramanian et al.[200] proposed a scheme to automatically identify and analyze microstructures in samples from 3D data. The technique does not require a priori description of the microstructure of the target system, is insensitive to disorder, and can quantitatively obtain unbiased microstructural information. They successfully applied the technique to simulation data and experimental characterization data of different materials, such as metals, polymers, and complex fluids, and conducted comparative studies with other methods. The method is computationally efficient and can quickly identify, track, and quantify complex microstructural features that affect material properties.

Chen et al.[201] proposed a short-term health state and remaining service life prediction method based on particle filter algorithm, and established a model, as shown in **Figure 8**a. Finally, the developed model and method are validated with $LiCoO_2$ and graphite half-cell cell data. The root mean square error and mean absolute error of the calculated voltages were kept within 38 and 51 mV. The root mean square errors of RUL and short-term SOH predictions were kept within 5.549 and 1.31%, respectively. Ruben et al.[202] proposed a graphical method based

on EIS reconstruction to demonstrate the degradation process of $LiCoO_2$ and the effect of chemical modification. Structural changes in $LiCoO_2$ mainly affected by intercalation were detected in the reconstruction of the Bode phase diagram in a specific frequency range, as shown in Figure 8b.

$LiCoO_2$ has important applications as a cathode material for aqueous lithium-ion batteries. Machine learning has also played an important role in the study of $LiCoO_2$.[24] For example, the electrochemical properties of $LiCoO_2$ can be predicted by machine learning simulation methods, providing guidance for novel battery designs.[203,204] The automatic identification and analysis of $LiCoO_2$ microstructure can be realized by using deep learning technology, thereby improving the efficiency and accuracy of material characterization.[205,206] In addition, machine learning can also be used to optimize the $LiCoO_2$ synthesis method to improve the performance and stability of the material.[207]

In summary, machine learning has broad application prospects in the characterization and regulation of material microstructures, and has played an important role in the research of $LiCoO_2$, a cathode material for water-based lithium-ion batteries. Through the method of machine learning, we can better understand the relationship between the microstructure and properties of materials, and provide strong support for the design and development of new materials.

6.3. Future Strategies of Machine Learning Methods in Optimizing $LiCoO_2$ Cathodes

Machine learning methods have great potential and strategies for future development in optimizing $LiCoO_2$ cathodes. $LiCoO_2$ is an important cathode material for lithium-ion batteries, and its performance directly affects the energy density and cycle life of batteries. However, traditional experimental and simulation methods have some limitations in material design and optimization, such as high cost, time-consuming, and complexity. The introduction of machine learning methods can effectively overcome these limitations and provide a faster, efficient and accurate optimization strategy.[208,209]

First of all, machine learning methods can quickly screen out $LiCoO_2$ cathode materials with potentially excellent performance by establishing a correlation model between material structure and performance. With a large amount of experimental data and computational results, highly accurate predictive models can be trained to provide targeted guidance in material design. This data-driven approach can greatly shorten the time for material screening and reduce the cost of testing.[210]

Second, machine learning methods can use optimization algorithms to find the best material composition and structural parameters. Through the automatic search and optimization of the structure of $LiCoO_2$ cathode materials, the key factors and optimization strategies hidden in the complex structure can be found. This machine learning-based optimization method can improve material performance and provide new ideas and directions for the design of new materials. Wang et al.[211] established a machine-learning interatomic potential model in the form of moment tensor potential, and screened interfacial coating materials for lithium-ion batteries with matching performance, as shown in **Figure 9a**. Combined with molecular dynamics simulations of its diffusion and trajectory at different temperatures Figure 9b,c. This approach identified two particularly promising materials for use as battery coatings, as well as several other candidates for doping to enhance ion conduction.

In addition, machine learning methods can also discover the correlation and regularity between materials by analyzing a large amount of material data and literature information. By mining these hidden laws and knowledge, deeper theoretical guidance can be provided for material design and optimization. This data-driven approach can help researchers better understand the nature of $LiCoO_2$ cathode materials and provide new ideas and directions for further research.

Machine learning methods have great potential in optimizing $LiCoO_2$ cathodes and strategies for future development.[212] By establishing association models, optimization algorithms, and data analysis, machine learning methods can provide faster, more efficient, and more accurate optimization strategies, providing new ideas and directions for performance improvement and material design of lithium-ion batteries.

Additionally, machine learning can also contribute to the optimization of high-voltage cathode materials, such as $LiCoO_2$.[206,213] As mentioned earlier, increasing the working voltage of $LiCoO_2$ can significantly improve its energy density. Machine learning algorithms can aid in the exploration of new strategies to enhance the stability and performance of $LiCoO_2$ under high-voltage conditions.[214] By analyzing the crystal structure, synthesis conditions, and surface/interface properties of $LiCoO_2$, machine learning models can identify key factors that influence its electrochemical performance. This knowledge can then be used to guide the development of better multi-strategy modification methods for $LiCoO_2$, ensuring its stability and improving its electrochemical performance.[215]

Furthermore, machine learning can assist in the design of high-pressure modification techniques for $LiCoO_2$.[216,217] By optimizing the crystal growth process, controlling grain size and stacking methods, and improving the chemical stability of the material's surface and interface, machine learning algorithms can help enhance the energy density, cycle life, and charge-discharge rate of $LiCoO_2$-based batteries.[218,219] Moreover, machine learning can aid in the selection and optimization of electrolytes and functional separators for high-voltage $LiCoO_2$ batteries.[220,221] By analyzing the interactions between the electrolyte, separator, and electrode materials, machine learning models can identify compatible combinations that improve the cycle stability and safety performance of the battery.[222,223] Looking towards the future, machine learning will continue to play a crucial role in advancing the field of materials research for aqueous lithium-ion batteries. As more data is generated and computational power increases, machine learning algorithms will become even more powerful in predicting material properties and guiding the design of new materials.[224,225]

In conclusion, machine learning has the potential to revolutionize the field of materials research for aqueous lithium-ion batteries. By leveraging the power of data analysis and prediction, machine learning can assist in the selection of electrode materials and the design of current collectors, ultimately leading to the development of more efficient and stable batteries. As research in this area progresses, it is expected that machine learning will

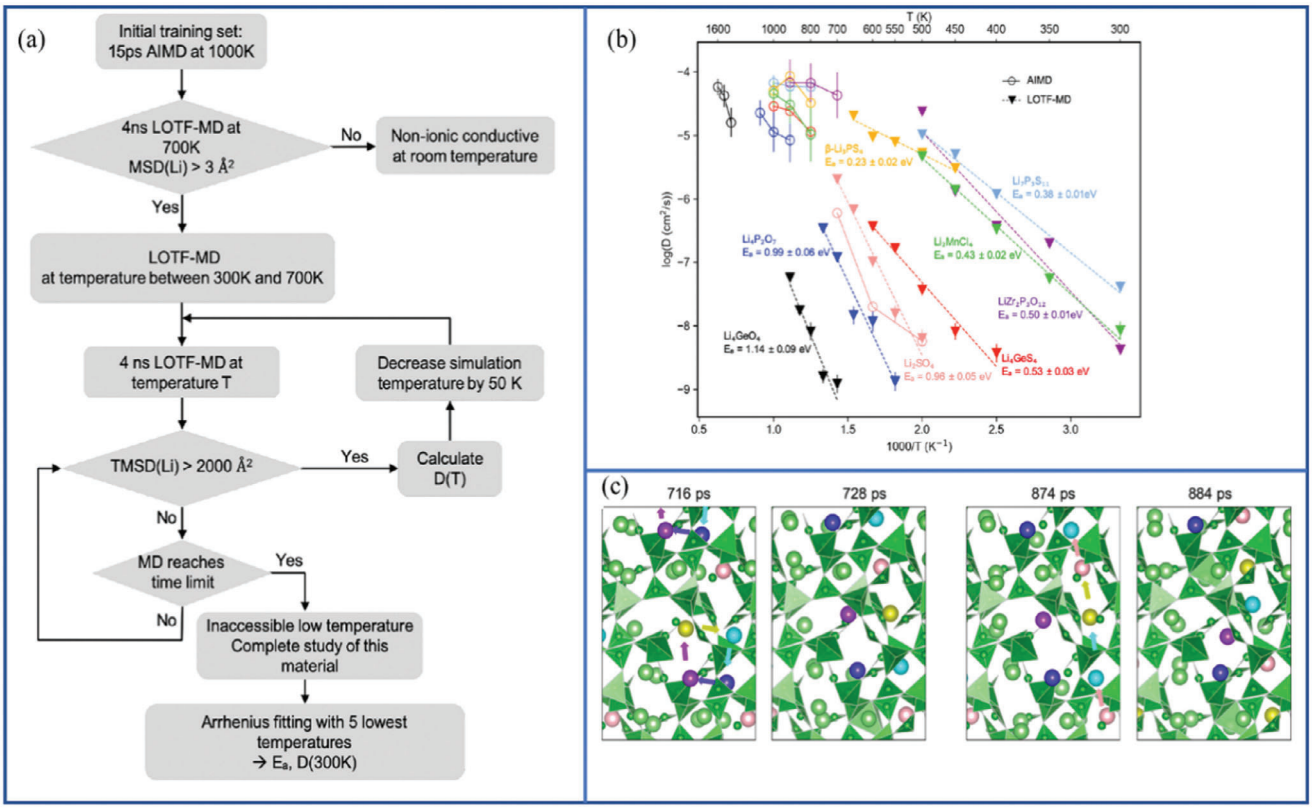

Figure 9. a) Flowchart of the screening process of LOTF-MD ionic conductors based on machine learning; b) the simulated diffusivity of AIMD at high temperature and LOTF-MD at intermediate temperatures on the Arrhenius diagram; c) Simulation Collective kinetic diffusion of Li^+ in $Li_3B_7O_{12}$ for LOTF-MD at 700 K. Reproduced with permission [211] Copyright 2020, American Chemical Society.

continue to play a crucial role in advancing the field of materials research for aqueous lithium-ion batteries.

However, there are some challenges and obstacles when developing machine learning models to optimize $LiCoO_2$ cathode materials:

1) Data acquisition and quality. Machine learning models require large amounts of high-quality data for training. For $LiCoO_2$ cathode materials, it may not be easy to obtain large-scale valid data. At the same time, ensuring the accuracy and reliability of the data is also a challenge, as determining the properties and characteristics of materials requires experimental testing and analysis.
2) Data diversity and reliability. Due to the complex chemical and structural properties of $LiCoO_2$ cathode materials, including electrical conductivity, ion diffusivity, crystal structure, etc., data variables covering multiple aspects are needed to build an accurate model. At the same time, these data should also be reliable to avoid the impact of noise and uncertainty on model training.
3) Model building and verification. Machine learning models for $LiCoO_2$ cathode materials need to have sufficient accuracy and credibility to provide practical conclusions and recommendations. To this end, it is necessary to correctly select the appropriate machine learning algorithm and modeling method, and conduct verification and verification experiments to evaluate the performance and reliability of the model.
4) Understanding of physics and chemistry. Machine learning models establish patterns and associations by learning from large amounts of data, but in-depth material science knowledge and domain expertise are still required to truly understand the physical and chemical mechanisms of $LiCoO_2$ cathode materials. Relying solely on machine learning models may not provide a thorough understanding of the nature of materials.
5) Experimental verification and application. Although machine learning models can provide important guidance and predictions, the final validation and application still requires experimental verification and practical application testing. Therefore, it is necessary to combine experiments and computer simulations to verify the predictive ability of the model and to apply the optimized materials to performance tests in actual battery systems.

In summary, the development of machine learning models to optimize $LiCoO_2$ cathode materials faces challenges and obstacles such as data acquisition and quality, data diversity and reliability, model establishment and verification, physical and chemical understanding, and experimental verification and application. Solving these problems requires a comprehensive consideration

of knowledge and technology in different fields, and a close combination of experiment and theory.

7. Summary and Outlook

As research and development in new energy vehicles advance and the commercialization of ternary cathodes expands, three key cathode materials $LiCoO_2$, $LiFePO_4$, and $LiMn_2O_4$ remain pivotal in hybrid vehicles, electric vehicles, and wearable electronic devices, particularly in the realm of aqueous lithium-ion batteries.[226] Reducing the production cost of lithium-ion batteries, improving energy density, and battery life are issues that need to be solved urgently. Most countries and companies have invested huge funds and manpower in improving energy density, but the research progress is relatively slow. Compared with traditional organic lithium-ion batteries, aqueous lithium-ion batteries have many advantages, but further research is still needed. Aqueous lithium-ion batteries have a unique cost advantage and belong to a new generation of clean energy. However, the road to development is not smooth, and it still faces many complex difficulties and challenges.[42,227,228]

The main problems faced by aqueous lithium-ion batteries are listed below: ① Compared with organic electrolytes, the stable electrochemical window of aqueous electrolytes is narrow. The decomposition of water (that is, the occurrence of oxygen evolution or hydrogen evolution phenomenon) must be considered when selecting electrode materials for aqueous lithium-ion batteries. Although there is an overpotential for hydrogen and oxygen evolution, the stable working voltage of a single positive or anode material is difficult to exceed 2 V. Typically full cells operate at approximately 1.3–2.0 V, or even lower.[229,230] Therefore, the selection range of electrode materials is relatively narrow. ②Compared with organic electrolytes, the non-electrochemical and electrochemical processes of lithium intercalation compounds in aqueous electrolyte systems are much more complex than those in organic systems, and will be accompanied by many side reactions.[231] For example, the side reactions caused by water and oxygen, the dissolution of electrode materials in aqueous solution and the structural changes of electrode materials during cycling, the competition between protons and lithium ions for intercalation in electrode materials, the hydrogen evolution/oxygen evolution reactions in inappropriate voltage ranges, and the interaction between electrode materials and water or oxygen reaction problem. ③ Compared with organic lithium-ion batteries, there are more factors to consider in the selection of water-based lithium-ion battery current collectors. How to prevent the oxidation and corrosion of the current collector to improve the effective life and cycle life of the battery needs to be solved urgently.[232,233] These challenges largely limit the development of aqueous lithium-ion batteries.

The direction of improving the performance of aqueous lithium-ion batteries and lithium-ion batteries in the future includes the following points:

1) Improvement of electrode materials: Improving positive and negative electrode materials is the key to improving the performance of aqueous lithium-ion batteries. New electrode materials with high ion transport rate and storage capacity can be searched for, such as the improvement of lithium cobaltate and the development of its alternative materials. In addition, exploring new anode materials, such as silicon-based materials, can improve the energy density of batteries.[66]
2) Electrolyte optimization: Improving the electrolyte of aqueous lithium-ion batteries is another key to improving performance. Electrolytes with high ionic conductivity, wide operating voltage window, and better interfacial stability need to be developed. For example, changing the chemical composition of the electrolyte by adding additives or lithium salts can improve the cycle stability and safety of the battery.[234,235]
3) Interface control and battery architecture design: By optimizing the battery interface structure and design, the performance of aqueous lithium-ion batteries can be improved. This includes optimizing the interface between the electrode material and the electrolyte, reducing the internal resistance of the battery and increasing the rate of ion transport. Meanwhile, designing appropriate battery architectures, such as micro/nanostructures and porous materials, can increase the surface area of electrode materials and improve the capacity and charge-discharge rate of batteries.[236]
4) Exploration of emerging technologies: Active exploration of emerging technologies, such as solid-state electrolytes, multi-ion transport, sodium sulfide, etc., can provide new ways to improve the performance of aqueous lithium-ion batteries. These technologies may improve the energy density, cycle life and safety performance of batteries.
5) System-level optimization: In addition to the improvement of individual battery components, optimizing the design of the entire battery system is an important step in improving performance. This can include improvements in the battery management system (BMS) to enable better charge and discharge control and ensure equalization of individual cells in the battery pack. In addition, system-level optimization is necessary considering the cost, weight, and volume of the battery.

In general, the key to improving the performance of aqueous lithium-ion batteries in the future lies in the improvement of materials, optimization of electrolytes, interface control and optimization of battery architecture design, and actively exploring emerging technologies. In addition, system-level optimization is also essential. The comprehensive application of these methods can improve the energy density, cycle life, safety and reliability of aqueous lithium-ion batteries, and promote their wide application in energy storage and electric vehicles.[237]

As one of the common cathode materials for aqueous lithium-ion batteries, it was found in the early research on lithium cobalt oxide materials that its working voltage must be within 4.25 V, otherwise the performance of lithium batteries will drop rapidly.[238] This is because at higher voltages, lithium cobalt oxide materials may undergo some side reactions, such as electrolytic decomposition of the electrolyte and release of oxygen, etc., resulting in decreased battery performance and increased safety risks. During the charging process, when the battery reaches a predetermined upper limit voltage (usually ≈4.2 V), the charging process needs to be stopped to avoid it exceeding the safe range and causing problems. Also, during the discharge process, it is recommended to limit the operating voltage of $LiCoO_2$ material to a lower value (such as 4.0 V) to ensure the stability and life of the battery. However, as the market

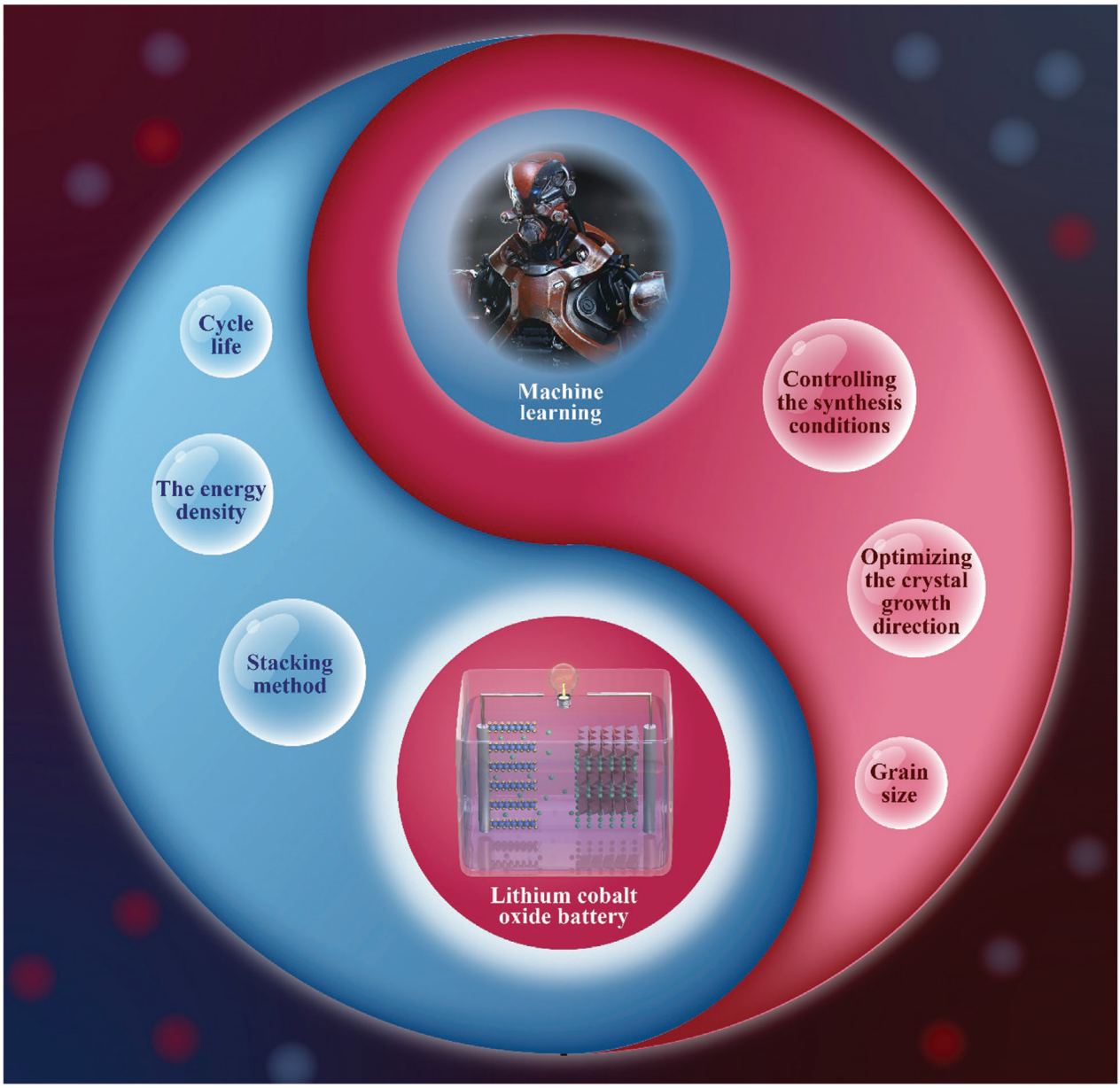

Figure 10. Development and application of aqueous lithium-ion batteries based on machine learning.

demand for lithium cobalt oxide battery industry is getting higher and higher, the topic of improving lithium cobalt oxide cathode materials, increasing their energy density and cycle life has gradually become the focus of current industry research. Theoretical studies have found that increasing the working voltage of lithium cobalt oxide can increase its energy density. In this regard, the researchers used surface coating and bulk doping optimization methods to improve the structural stability of lithium cobalt oxide. It is guaranteed that under high working voltage, the layered structure of lithium cobalt oxide can adapt to the change of voltage, maintain the stability of the structure, and improve the electrochemical performance of the material[239]. However, there is still no clear conclusion on how to construct highly stable and high-$LiCoO_2$ materials through a better multi-strategy synergistic modification method, and further research is needed.

One potential solution to address these challenges is the application of machine learning techniques in materials research. Machine learning has shown great potential in accelerating the discovery and optimization of materials, and it can play a significant role in advancing the development of aqueous lithium-ion batteries.[240] Machine learning algorithms can analyze large amounts of experimental and computational data to identify patterns and relationships that are difficult for humans to discern. By training models on existing data, machine learning algorithms can predict the properties and performance of new materials, enabling researchers to make informed decisions on which materials to synthesize and test[241] as shown in **Figure 10**.

In the context of aqueous lithium-ion batteries, machine learning can be used to predict the stability and electrochemical performance of electrode materials in aqueous electrolytes.[242] By considering factors such as water decomposition, side reactions, and competition between protons and lithium ions, machine learning models can guide the selection of electrode materials with improved stability and performance. Furthermore, machine learning can also assist in the design of current collectors for aqueous lithium-ion batteries.[243] By analyzing the properties and behavior of different materials, machine learning algorithms can identify materials that are resistant to oxidation and corrosion, thus improving the overall lifespan and cycle life of the battery.[244,245] Looking ahead, the integration of machine learning and materials research holds great promise for the development of aqueous lithium-ion batteries. As more data becomes available and machine learning algorithms become more sophisticated, researchers will be able to make more accurate predictions and design materials with enhanced properties.

At present, with the continuous deepening of the research on the structure of high-voltage lithium cobalt oxide cathode materials, it has been found that the high-pressure modification design of lithium cobalt oxide does not only require re-optimization of the crystal structure of the design material. Factors affecting its comprehensive performance also include controlling the molding process of crystal growth and improving the chemical stability of the surface and interface of lithium cobalt oxide materials.[246] For example, by controlling the synthesis conditions and optimizing the crystal growth direction, grain size, and stacking method, the energy density, cycle life, and charge-discharge rate of the battery can be improved.[247]

By improving the chemical stability of the surface and interface of the material, the high-temperature storage performance and safety performance of the material can be improved. In addition to the above performance improvement methods, the matching use of high-voltage electrolyte and functional diaphragm is also an effective means to improve the cycle stability of materials. This is also an important means for the high-voltage design of commercial lithium cobalt oxide materials in the future. After further research on lithium cobalt oxide in the future, the theoretical capacity and working voltage limit of lithium cobalt oxide will be substantially improved and improved. It is believed that these performance and application problems can be solved one by one on the road of future research.[248] According to the above research results, some inspiration can be obtained from it, and it can be applied to the water system to solve the current problems of lithium cobalt oxide.

Due to the large-scale mining of Co and the political turmoil in Africa, the cost of Co-containing cathodes has further increased. Conventional $LiCoO_2$ cathodes are no longer suitable for current commercial battery systems. Increasing the content of Ni in the positive electrode and reducing or even eliminating Co has gradually become the current research and development trend.

Acknowledgements

H.M and F.W. contributed equally to this work. H. Hu thanks the support from Scientific Research Startup Fund for Shenzhen High-Caliber Personnel of Shenzhen Polytechnic (No. 6022310038k).

Conflict of Interest

The authors declare no conflict of interest.

Keywords

aqueous lithium-ion battery, attenuation mechanism, cathode material, $LiCoO_2$, machine learning

Received: June 30, 2023
Revised: December 1, 2023
Published online:

[1] T. Kim, W. Song, D.-Y. Son, L. K. Ono, Y. Qi, *J. Mater. Chem. A* **2019**, *7*, 2942.
[2] M. Li, J. Lu, Z. Chen, K. Amine, *Adv. Mater.* **2018**, *30*, 1800561.
[3] J. Xie, Y.-C. Lu, *Nat. Commun.* **2020**, *11*, 2499.
[4] G. E. Blomgren, *J. Electrochem. Soc.* **2016**, *164*, A5019.
[5] W. Van Schalkwijk, B. Scrosati, in *Advances in lithium ion batteries introduction*, Springer, Berlin, Germany **2002**.
[6] A. Von Wald Cresce, K. Xu, *Carbon Energy* **2021**, *3*, 721.
[7] D. Bin, Y. Wen, Y. Wang, Y. Xia, *J. Energy Chem.* **2018**, *27*, 1521.
[8] C. Yang, J. Chen, T. Qing, X. Fan, W. Sun, A. Von Cresce, M. S. Ding, O. Borodin, J. Vatamanu, M. A. Schroeder, N. Eidson, C. Wang, K. Xu, *Joule* **2017**, *1*, 122.
[9] S. Li, K. Wang, G. Zhang, S. Li, Y. Xu, X. Zhang, X. Zhang, S. Zheng, X. Sun, Y. Ma, *Adv. Funct. Mater.* **2022**, *32*, 2200796.
[10] X. Li, X. Sun, X. Hu, F. Fan, S. Cai, C. Zheng, G. D. Stucky, *Nano Energy* **2020**, *77*, 105143.
[11] M. A. Azam, N. E. Safie, A. S. Ahmad, N. A. Yuza, N. S. A. Zulkifli, *J. Energy Storage* **2021**, *33*, 102096.
[12] H. Cheng, J. G. Shapter, Y. Li, G. Gao, *J. Energy Chem.* **2021**, *57*, 451.
[13] Y. Lyu, X. Wu, K. Wang, Z. Feng, T. Cheng, Y. Liu, M. Wang, R. Chen, L. Xu, J. Zhou, Y. Lu, B. Guo, *Adv. Energy Mater.* **2021**, *11*, 2000982.
[14] E. Paccha-Herrera, W. R. Calderón-Muñoz, M. Orchard, F. Jaramillo, K. Medjaher, *Batteries* **2020**, *6*, 40.
[15] R. Tao, P. Xing, H. Li, Z. Sun, Y. Wu, *Resour., Conserv. Recycl.* **2022**, *176*, 105921.
[16] X. Liu, Y. Tan, W. Wang, C. Li, Z. W. Seh, L. Wang, Y. Sun, *Nano Lett.* **2020**, *20*, 4558.
[17] J.-C. Zhang, Z.-D. Liu, C.-H. Zeng, J.-W. Luo, Y.-D. Deng, X.-Y. Cui, Y.-N. Chen, *Rare Met.* **2022**, *41*, 3946.
[18] L. Suo, O. Borodin, T. Gao, M. Olguin, J. Ho, X. Fan, C. Luo, C. Wang, K. Xu, *Science* **2015**, *350*, 938.
[19] S.-D. Zhang, M.-Y. Qi, S.-J. Guo, Y.-G. Sun, X.-X. Tan, P.-Z. Ma, J.-Y. Li, R.-Z. Yuan, A.-M. Cao, L.-J. Wan, *Small Methods* **2022**, *6*, 2200148.
[20] S. Mao, Z. Shen, W. Zhang, Q. Wu, Z. Wang, Y. Lu, *Adv. Sci.* **2022**, *9*, 2104841.
[21] W. Zhang, F. H. Richter, S. P. Culver, T. Leichtweiss, J. G. Lozano, C. Dietrich, P. G. Bruce, W. G. Zeier, J. Janek, *ACS Appl. Mater. Interfaces* **2018**, *10*, 22226.
[22] J. Wang, Z. Liang, Y. Zhao, J. Sheng, J. Ma, K. Jia, B. Li, G. Zhou, H.-M. Cheng, *Energy Storage Mater.* **2022**, *45*, 768.
[23] S. S. Choi, H. S. Lim, *J. Power Sources* **2002**, *111*, 130.
[24] M. Hong, S. Lee, V.-C. Ho, D. Lee, S.-H. Yu, J. Mun, *ACS Appl. Mater. Interfaces* **2022**, *14*, 10267.
[25] R. Ruffo, C. Wessells, R. A. Huggins, Y. Cui, *Electrochem. Commun.* **2009**, *11*, 247.
[26] J. R. Dahn, U. Von Sacken, M. W. Juzkow, H. Al-Janaby, *J. Electrochem. Soc.* **1991**, *138*, 2207.
[27] C. H. Mi, X. G. Zhang, H. L. Li, *J. Electroanal. Chem.* **2007**, *602*, 245.
[28] F. Huet, *J. Power Sources* **1998**, *70*, 59.

[29] A. A. Mohamad, *Corros. Sci.* **2008**, *50*, 3475.
[30] N. Alias, A. A. Mohamad, *J. Power Sources* **2015**, *274*, 237.
[31] Z. Li, X. Feng, L. Mi, J. Zheng, X. Chen, W. Chen, *Nano Res.* **2018**, *11*, 4038.
[32] M. Baumung, L. Kollenbach, L. Xi, M. Risch, *ChemPhysChem* **2019**, *20*, 2981.
[33] W. Li, J. R. Dahn, D. S. Wainwright, *Science* **1994**, *264*, 1115.
[34] J. Zhang, L. Zhang, H. Liu, A. Sun, R.-S. Liu, in *Electrochemical Technologies for Energy Storage and Conversion, 2 Volume Set*, John Wiley & Sons, Hoboken, New Jersey **2011**.
[35] K. E. Aifantis, S. A. Hackney, in *High Energy Density Lithium Batteries: Materials, Engineering, Applications*, **2010**, pp. 81–101.
[36] Y. Li, J. Song, J. Yang, *Renew. Sustain. Energy Rev.* **2014**, *37*, 627.
[37] X. Chen, Q. Zhang, *Acc. Chem. Res.* **2020**, *53*, 1992.
[38] X. Fan, C. Wang, *Chem. Soc. Rev.* **2021**, *50*, 10486.
[39] Y. Hu, Y. Ren, R. Shi, J. Yu, Z. Sun, S. Guo, J. Guo, F. Yan, *ACS Appl. Mater. Interfaces* **2021**, *13*, 16289.
[40] Q. Ni, B. Kim, C. Wu, K. Kang, *Adv. Mater.* **2022**, *34*, 2108206.
[41] J. Shin, J. W. Choi, *Adv. Energy Mater.* **2020**, *10*, 2001386.
[42] S. Ko, Y. Yamada, K. Miyazaki, T. Shimada, E. Watanabe, Y. Tateyama, T. Kamiya, T. Honda, J. Akikusa, A. Yamada, *Electrochem. Commun.* **2019**, *104*, 106488.
[43] A. El Kharbachi, O. Zavorotynska, M. Latroche, F. Cuevas, V. Yartys, M. Fichtner, *J. Alloys Compd.* **2020**, *817*, 153261.
[44] L. Xue, Q. Zhang, X. Zhu, L. Gu, J. Yue, Q. Xia, T. Xing, T. Chen, Y. Yao, H. Xia, *Nano Energy* **2019**, *56*, 463.
[45] M. Pagliaro, F. Meneguzzo, *Heliyon* **2019**, 5, e01866.
[46] J. Neumann, M. Petranikova, M. Meeus, J. D. Gamarra, R. Younesi, M. Winter, S. Nowak, *Adv. Energy Mater.* **2022**, *12*, 2102917.
[47] Q. Wang, P. Ping, X. Zhao, G. Chu, J. Sun, C. Chen, *J. Power Sources* **2012**, *208*, 210.
[48] B. Scrosati, J. Hassoun, Y.-K. Sun, *Energy Environ. Sci.* **2011**, *4*, 3287.
[49] M. Yoshio, R. J. Brodd, A. Kozawa, in *Lithium-ion batteries*, Springer, Berlin, Germany **2009**.
[50] D. Aurbach, Y. Talyosef, B. Markovsky, E. Markevich, E. Zinigrad, L. Asraf, J. S. Gnanaraj, H.-J. Kim, *Electrochim. Acta* **2004**, *50*, 247.
[51] G. Xu, Z. Liu, C. Zhang, G. Cui, L. Chen, *J. Mater. Chem. A* **2015**, *3*, 4092.
[52] L. Lu, X. Han, J. Li, J. Hua, M. Ouyang, *J. Power Sources* **2013**, *226*, 272.
[53] D. P. Abraham, E. P. Roth, R. Kostecki, K. Mccarthy, S. Maclaren, D. H. Doughty, *J. Power Sources* **2006**, *161*, 648.
[54] Y. Hou, X. Wang, Y. Zhu, C. Hu, Z. Chang, Y. Wu, R. Holze, *J. Mater. Chem. A* **2013**, *1*, 14713.
[55] Y. Meng, Y. Yang, *Electrochem. Commun.* **2007**, *9*, 1428.
[56] D. Saikia, Y.-H. Chen, Y.-C. Pan, J. Fang, L.-D. Tsai, G. T. K. Fey, H.-M. Kao, *J. Mater. Chem.* **2011**, *21*, 10542.
[57] P. Barbosa, L. Rodrigues, M. Silva, M. Smith, A. Gonçalves, E. Fortunato, *J. Mater. Chem.* **2010**, *20*, 723.
[58] M. C. López, G. F. Ortiz, E. M. Arroyo-De Dompablo, J. L. Tirado, *Inorg. Chem.* **2014**, *53*, 2310.
[59] R. Ruffo, F. La Mantia, C. Wessells, R. A. Huggins, Y. Cui, *Solid State Ionics* **2011**, *192*, 289.
[60] X.-H. Liu, T. Saito, T. Doi, S. Okada, J.-I. Yamaki, *J. Power Sources* **2009**, *189*, 706.
[61] X. Hou, X. Liu, H. Wang, X. Zhang, J. Zhou, M. Wang, *Energy Storage Mater.* **2023**, *57*, 577.
[62] H. Jia, Z. Wang, B. Tawiah, Y. Wang, C.-Y. Chan, B. Fei, F. Pan, *Nano Energy* **2020**, *70*, 104523.
[63] Y. Yamada, J. Wang, S. Ko, E. Watanabe, A. Yamada, *Nat. Energy* **2019**, *4*, 269.
[64] T. Liang, R. Hou, Q. Dou, H. Zhang, X. Yan, *Adv. Funct. Mater.* **2021**, *31*, 2006749.
[65] J. Billaud, F. Bouville, T. Magrini, C. Villevieille, A. R. Studart, *Nat. Energy* **2016**, *1*, 16097.
[66] D. Chao, W. Zhou, F. Xie, C. Ye, H. Li, M. Jaroniec, S.-Z. Qiao, *Sci. Adv.* **2020**, *6*, eaba4098.
[67] C. Xu, Z. Yang, X. Zhang, M. Xia, H. Yan, J. Li, H. Yu, L. Zhang, J. Shu, *Nano-Micro Lett.* **2021**, *13*, 166.
[68] H. Wang, J. F. Whitacre, *Energy Technol.* **2018**, *6*, 2429.
[69] H. Seki, K. Yoshima, Y. Yamashita, S. Matsuno, N. Takami, *J. Power Sources* **2021**, *482*, 228950.
[70] M. Abdollahifar, S.-S. Huang, Y.-H. Lin, H.-S. Sheu, J.-F. Lee, M.-L. Lu, Y.-F. Liao, N.-L. Wu, *J. Power Sources* **2019**, *412*, 545.
[71] T. Xue, H. J. Fan, *J. Energy Chem.* **2021**, *54*, 194.
[72] Z. Liu, L. Qin, B. Lu, X. Wu, S. Liang, J. Zhou, *ChemSusChem* **2022**, *15*, 202200348.
[73] J. Shin, J. K. Seo, R. Yaylian, A. Huang, Y. S. Meng, *Int. Mater. Rev.* **2020**, *65*, 356.
[74] Y. Zhou, W. Shan, S. Wang, K.-H. Lam, Q. Ru, F. Chen, X. Hou, *Electrochim. Acta* **2020**, *332*, 135529.
[75] H. Oh, S.-J. Shin, E. Choi, H. Yamagishi, T. Ohta, N. Yabuuchi, H.-G. Jung, H. Kim, H. R. Byon, *JACS Au* **2023**, *3*, 1392.
[76] M. Kunduraci, S. K. Cetin, U. Caglayan, R. N. Mutlu, D. Kaya, A. Ekicibil, *J. Electroanal. Chem.* **2022**, *908*, 116118.
[77] Y. Li, X. Hou, Y. Zhou, W. Han, C. Liang, X. Wu, S. Wang, Q. Ru, *Energy Technol.* **2018**, *6*, 391.
[78] A. Tron, S. Jeong, Y. D. Park, J. Mun, *ACS Sustain. Chem. Eng.* **2019**, *7*, 14531.
[79] S. Lee, J. Jang, D. Lee, J. Kim, J. Mun, *Int. J. Energy Res.* **2022**, *46*, 6480.
[80] Z. Zhang, M. Avdeev, H. Chen, W. Yin, W. H. Kan, G. He, *Nat. Commun.* **2022**, *13*, 7790.
[81] M. J. P. Muñoz, E. C. Martínez, in *Prussian blue based batteries*, Springer, Berlin, Germany **2018**.
[82] Y. Song, T. Wang, J. Zhu, Y. Liu, L. Wang, L. Dai, Z. He, *J. Alloys Compd.* **2022**, *897*, 163065.
[83] Y. Rublova, R. Meija, V. Lazarenko, J. Andzane, J. Svirksts, D. Erts, *Batteries* **2023**, *9*, 260.
[84] Z. Wang, T. Huang, Z. Liu, A. Yu, *Electrochim. Acta* **2021**, *389*, 138806.
[85] Z. Zhang, D. Wu, L. Jiang, F. Liang, Y. Rui, B. Tang, *J. Alloys Compd.* **2022**, *899*, 163274.
[86] Z. Huang, M. Yao, Z. Jiang, W. Meng, B. Li, C. Li, C. Li, Z. He, W. Meng, L. Dai, L. Wang, *Solid State Ionics* **2018**, *327*, 123.
[87] Y. Dong, L. Wang, S. Zhang, Y. Zhao, J. Zhou, H. Xie, J. B. Goodenough, *J. Power Sources* **2012**, *215*, 116.
[88] K. Zhang, J. Cao, S. Tian, H. Guo, R. Liu, X. Ren, L. Wen, G. Liang, *Ionics* **2021**, *27*, 4629.
[89] K.-S. Park, P. Xiao, S.-Y. Kim, A. Dylla, Y.-M. Choi, G. Henkelman, K. J. Stevenson, J. B. Goodenough, *Chem. Mater.* **2012**, *24*, 3212.
[90] Y.-H. Huang, K.-S. Park, J. B. Goodenough, *J. Electrochem. Soc.* **2006**, *153*, A2282.
[91] C. Sun, S. Rajasekhara, J. B. Goodenough, F. Zhou, *J. Am. Chem. Soc.* **2011**, *133*, 2132.
[92] K. L. Harrison, C. A. Bridges, M. P. Paranthaman, C. U. Segre, J. Katsoudas, V. A. Maroni, J. C. Idrobo, J. B. Goodenough, A. Manthiram, *Chem. Mater.* **2013**, *25*, 768.
[93] K. Numata, *Solid State Ionics* **1999**, *117*, 257.
[94] M. Manickam, P. Singh, S. Thurgate, K. Prince, *J. Power Sources* **2006**, *158*, 646.
[95] P. He, J.-L. Liu, W.-J. Cui, J.-Y. Luo, Y.-Y. Xia, *Electrochim. Acta* **2011**, *56*, 2351.
[96] L.-X. Yuan, Z.-H. Wang, W.-X. Zhang, X.-L. Hu, J.-T. Chen, Y.-H. Huang, J. B. Goodenough, *Energy Environ. Sci.* **2011**, *4*, 269.
[97] H. Porthault, R. Baddour-Hadjean, F. Le Cras, C. Bourbon, S. Franger, *Vib. Spectrosc.* **2012**, *62*, 152.

[98] H. Xia, Z. Luo, J. Xie, *Prog. Nat. Sci.: Mater. Int.* **2012**, *22*, 572.
[99] P. Nie, L. Shen, H. Luo, B. Ding, G. Xu, J. Wang, X. Zhang, *J. Mater. Chem. A* **2014**, *2*, 5852.
[100] H. Chen, C. P. Grey, *Adv. Mater.* **2008**, *20*, 2206.
[101] J. Kemp, P. Cox, *J. Phys.: Condens. Matter* **1990**, *2*, 9653.
[102] J. Kikkawa, T. Akita, M. Tabuchi, M. Shikano, K. Tatsumi, M. Kohyama, *Electrochem. Solid-State Lett.* **2008**, *11*, A183.
[103] K. Sekai, H. Azuma, A. Omaru, S. Fujita, H. Imoto, T. Endo, K. Yamaura, Y. Nishi, S. Mashiko, M. Yokogawa, *J. Power Sources* **1993**, *43*, 241.
[104] C. Delmas, J.-J. Braconnier, P. Hagenmuller, *Mater. Res. Bull.* **1982**, *17*, 117.
[105] S. Al Hallaj, J. Prakash, J. R. Selman, *J. Power Sources* **2000**, *87*, 186.
[106] W. Tang, L. L. Liu, S. Tian, L. Li, Y. B. Yue, Y. P. Wu, S. Y. Guan, K. Zhu, *Electrochem. Commun.* **2010**, *12*, 1524.
[107] S. Fritsch, J. E. Post, A. Navrotsky, *Geochim. Cosmochim. Acta* **1997**, *61*, 2613.
[108] X. Huang, D. Lv, H. Yue, A. Attia, Y. Yang, *Nanotechnology* **2008**, *19*, 225606.
[109] Q.-Z. Zhang, D. Zhang, Z.-C. Miao, X.-L. Zhang, S.-L. Chou, *Small* **2018**, *14*, 1702883.
[110] M. Zhang, Y. Chen, D. Yang, J. Li, *J. Energy Storage* **2020**, *29*, 101363.
[111] R. L. Deutscher, T. M. Florence, R. Woods, *J. Power Sources* **1995**, *55*, 41.
[112] A. Yuan, Q. Zhang, *Electrochem. Commun.* **2006**, *8*, 1173.
[113] Q. Qu, P. Zhang, B. Wang, Y. Chen, S. Tian, Y. Wu, R. Holze, *J. Phys. Chem. C* **2009**, *113*, 14020.
[114] Y. Gao, H. Yang, Y. Bai, C. Wu, *J. Mater. Chem. A* **2021**, *9*, 11472.
[115] L. Tian, A. Yuan, *J. Power Sources* **2009**, *192*, 693.
[116] Z. Iskandar Radzi, K. Helmy Arifin, M. Zieauddin Kufian, V. Balakrishnan, S. Rohani Sheikh Raihan, N. Abd Rahim, R. Subramaniam, *J. Electroanal. Chem.* **2022**, 116623.
[117] J. Abou-Rjeily, I. Bezza, N. A. Laziz, C. Autret-Lambert, M. T. Sougrati, F. Ghamouss, *Energy Storage Mater.* **2020**, *26*, 423.
[118] Y.-G. Wang, Y.-Y. Xia, *J. Electrochem. Soc.* **2006**, *153*, A450.
[119] C. D. Wessells, S. V. Peddada, M. T. Mcdowell, R. A. Huggins, Y. Cui, *J. Electrochem. Soc.* **2011**, *159*, A98.
[120] C. Delmas, C. Fouassier, P. Hagenmuller, *Physica B+ c* **1980**, *99*, 81.
[121] M. G. S. R. Thomas, P. G. Bruce, J. B. Goodenough, *J. Electrochem. Soc.* **1985**, *132*, 1521.
[122] A. Van Der Ven, G. Ceder, *J. Power Sources* **2001**, *97*, 529.
[123] M. Nishizawa, S. Yamamura, *Chem. Commun.* **1998**, 1631.
[124] R. V. Chebiam, F. Prado, A. Manthiram, *Chem. Mater.* **2001**, *13*, 2951.
[125] S. Kalluri, M. Yoon, M. Jo, S. Park, S. Myeong, J. Kim, S. X. Dou, Z. Guo, J. Cho, *Adv. Energy Mater.* **2017**, *7*, 1601507.
[126] I. A. Courtney, J. R. Dahn, *J. Electrochem. Soc.* **1997**, *144*, 2045.
[127] G. G. Amatucci, J. M. Tarascon, L. C. Klein, *J. Electrochem. Soc.* **1996**, *143*, 1114.
[128] A. Van Der Ven, M. K. Aydinol, G. Ceder, G. Kresse, J. Hafner, *Phys. Rev. B* **1998**, *58*, 2975.
[129] K. Mizushima, P. Jones, P. Wiseman, J. Goodenough, *Solid State Ionics* **1981**, *3*, 171.
[130] J. Qian, L. Liu, J. Yang, S. Li, X. Wang, H. L. Zhuang, Y. Lu, *Nat. Commun.* **2018**, *9*, 4918.
[131] J. N. Reimers, J. R. Dahn, *J. Electrochem. Soc.* **1992**, *139*, 2091.
[132] S. A. Needham, G. X. Wang, H. K. Liu, V. A. Drozd, R. S. Liu, *J. Power Sources* **2007**, *174*, 828.
[133] A. Liu, J. Li, R. Shunmugasundaram, J. R. Dahn, *J. Electrochem. Soc.* **2017**, *164*, A1655.
[134] Y. Jin, S. Xu, Z. Li, K. Xu, W. Ding, J. Song, H. Wang, J. Zhao, *J. Electrochem. Soc.* **2018**, *165*, A2267.
[135] F.-E. Er-Rami, M. Duffiet, S. Hinkle, J. Auvergniot, M. Blangero, P.-E. Cabelguen, K. Song, F. Weill, C. Delmas, D. Carlier, *Chem. Mater.* **2022**, *34*, 4384.
[136] S. Zhou, Z. Fei, Q. Meng, P. Dong, Y. Zhang, M. Zhang, *ACS Appl. Energy Mater.* **2021**, *4*, 12677.
[137] Y. Deng, T. Kang, Z. Ma, X. Tan, X. Song, Z. Wang, P. Pang, D. Shu, X. Zuo, J. Nan, *Electrochim. Acta* **2019**, *295*, 703.
[138] Y. Wang, Q. Zhang, Z.-C. Xue, L. Yang, J. Wang, F. Meng, Q. Li, H. Pan, J.-N. Zhang, Z. Jiang, W. Yang, X. Yu, L. Gu, H. Li, *Adv. Energy Mater.* **2020**, *10*, 2001413.
[139] P. Pang, Z. Wang, Y. Deng, J. Nan, Z. Xing, H. Li, *ACS Appl. Mater. Interfaces* **2020**, *12*, 27339.
[140] Q. Liu, X. Su, D. Lei, Y. Qin, J. Wen, F. Guo, Y. A. Wu, Y. Rong, R. Kou, X. Xiao, F. Aguesse, J. Bareño, Y. Ren, W. Lu, Y. Li, *Nat. Energy* **2018**, *3*, 936.
[141] D. Qian, Y. Hinuma, H. Chen, L.-S. Du, K. J. Carroll, G. Ceder, C. P. Grey, Y. S. Meng, *J. Am. Chem. Soc.* **2012**, *134*, 6096.
[142] R. V. Chebiam, A. M. Kannan, F. Prado, A. Manthiram, *Electrochem. Commun.* **2001**, *3*, 624.
[143] S. Venkatraman, Y. Shin, A. Manthiram, *Electrochem. Solid-State Lett.* **2002**, *6*, A9.
[144] J. Kikkawa, S. Terada, A. Gunji, T. Nagai, K. Kurashima, K. Kimoto, *J. Phys. Chem. C* **2015**, *119*, 15823.
[145] L. Yu, H. Liu, Y. Wang, N. Kuwata, M. Osawa, J. Kawamura, S. Ye, *Angew. Chem., Int. Ed.* **2013**, *22*, 5753.
[146] D. Takamatsu, Y. Koyama, Y. Orikasa, S. Mori, T. Nakatsutsumi, T. Hirano, H. Tanida, H. Arai, Y. Uchimoto, Z. Ogumi, *Angew. Chem., Int. Ed.* **2012**, *51*, 11597.
[147] S. Lin, J. Zhao, *ACS Appl. Mater. Interfaces* **2020**, *12*, 8316.
[148] L. Wang, J. Ma, C. Wang, X. Yu, R. Liu, F. Jiang, X. Sun, A. Du, X. Zhou, G. Cui, *Adv. Sci.* **2019**, *6*, 1900355.
[149] S. Wu, Y. Lin, L. Xing, G. Sun, H. Zhou, K. Xu, W. Fan, L. Yu, W. Li, *ACS Appl. Mater. Interfaces* **2019**, *11*, 17940.
[150] J.-N. Zhang, Q. Li, C. Ouyang, X. Yu, M. Ge, X. Huang, E. Hu, C. Ma, S. Li, R. Xiao, W. Yang, Y. Chu, Y. Liu, H. Yu, X.-Q. Yang, X. Huang, L. Chen, H. Li, *Nat. Energy* **2019**, *4*, 594.
[151] S. Sharifi-Asl, F. A. Soto, T. Foroozan, M. Asadi, Y. Yuan, R. Deivanayagam, R. Rojaee, B. Song, X. Bi, K. Amine, J. Lu, A. Salehi-Khojin, P. B. Balbuena, R. Shahbazian-Yassar, *Adv. Funct. Mater.* **2019**, *29*, 1901110.
[152] D. Carlier, *Solid State Ionics* **2001**, *144*, 263.
[153] D. Carlier, L. Croguennec, G. Ceder, M. Ménétrier, Y. Shao-Horn, C. Delmas, *Inorg. Chem.* **2004**, *43*, 914.
[154] S. Kim, V. I. Hegde, Z. Yao, Z. Lu, M. Amsler, J. He, S. Hao, J. R. Croy, E. Lee, M. M. Thackeray, *ACS Appl. Mater. Interfaces* **2018**, *10*, 13479.
[155] A. Mendiboure, C. Delmas, P. Hagenmuller, *Mater. Res. Bull.* **1984**, *19*, 1383.
[156] J. M. Paulsen, J. R. Mueller-Neuhaus, J. R. Dahn, *J. Electrochem. Soc.* **2000**, *147*, 508.
[157] Y. Shao-Horn, F. Weill, L. Croguennec, D. Carlier, M. Ménétrier, C. Delmas, *Chem. Mater.* **2003**, *15*, 2977.
[158] D. Carlier, A. Van der Ven, G. Ceder, L. Croguennec, M. Ménétrier, C. Delmas, *MRS Online Proceedings Library (OPL)* **2002**, *756*, EE5.9.
[159] J. M. Paulsen, C. L. Thomas, J. R. Dahn, *J. Electrochem. Soc.* **2000**, *147*, 861.
[160] Y. Zuo, B. Li, N. Jiang, W. Chu, H. Zhang, R. Zou, D. Xia, *Adv. Mater.* **2018**, *30*, 1707255.
[161] R. Gummow, M. Thackeray, W. David, S. Hull, *Mater. Res. Bull.* **1992**, *27*, 327.
[162] E. Rossen, J. Reimers, J. Dahn, *Solid State Ionics* **1993**, *62*, 53.
[163] S.-L. Cui, Y.-Y. Wang, S. Liu, G.-R. Li, X.-P. Gao, *Electrochim. Acta* **2019**, *328*, 135109.
[164] J. Wang, Q. Zhang, J. Sheng, Z. Liang, J. Ma, Y. Chen, G. Zhou, H.-M. Cheng, *Natl. Sci. Rev.* **2022**, *9*, nwac097.
[165] Q. Yang, J. Huang, Y. Li, Y. Wang, J. Qiu, J. Zhang, H. Yu, X. Yu, H. Li, L. Chen, *J. Power Sources* **2018**, *388*, 65.

[166] B. Hu, X. Lou, C. Li, F. Geng, C. Zhao, J. Wang, M. Shen, B. Hu, *J. Power Sources* **2019**, *438*, 226954.
[167] Z. Wang, Z. Wang, H. Guo, W. Peng, X. Li, G. Yan, J. Wang, *J. Alloys Compd.* **2015**, *621*, 212.
[168] F. Ning, B. Xu, J. Shi, M. Wu, Y. Hu, C. Ouyang, *J. Phys. Chem. C* **2016**, *120*, 18428.
[169] M. Zhu, Y. Huang, G. Chen, M. Lu, A. A. Nevar, N. Dudko, L. Shi, L. Huang, N. V Tarasenko, D. Zhang, *Chem. Eng. J.* **2023**, 143585.
[170] N. A. Abdul Aziz, T. K. Abdullah, A. A. Mohamad, *Ionics* **2018**, *24*, 403.
[171] Y. Liu, S. Gao, R. Holze, *Russ. J. Electrochem.* **2019**, *55*, 1068.
[172] P. Man, B. He, Q. Zhang, C. Li, Z. Zhou, Q. Li, W. Xu, G. Hong, Y. Yao, *ACS Appl. Mater. Interfaces* **2020**, *12*, 25700.
[173] G. J. Wang, Q. T. Qu, B. Wang, Y. Shi, S. Tian, Y. P. Wu, R. Holze, *Electrochim. Acta* **2009**, *54*, 1199.
[174] N. A. Abdul Aziz, M. De Cunha, T. K. Abdullah, A. A. Mohamad, *Int. J. Energy Res.* **2017**, *41*, 289.
[175] P. Jaumaux, X. Yang, B. Zhang, J. Safaei, X. Tang, D. Zhou, C. Wang, G. Wang, *Angew. Chem., Int. Ed.* **2021**, *60*, 19965.
[176] Z. Liu, H. Li, M. Zhu, Y. Huang, Z. Tang, Z. Pei, Z. Wang, Z. Shi, J. Liu, Y. Huang, C. Zhi, *Nano Energy* **2018**, *44*, 164.
[177] Y. Shang, N. Chen, Y. Li, S. Chen, J. Lai, Y. Huang, W. Qu, F. Wu, R. Chen, *Adv. Mater.* **2020**, *32*, 2004017.
[178] X. Gu, J.-L. Liu, J.-H. Yang, H.-J. Xiang, X.-G. Gong, Y.-y. Xia, *J. Phys. Chem. C* **2011**, *115*, 12672.
[179] M. Shao, J. Deng, F. Zhong, Y. Cao, X. Ai, J. Qian, H. Yang, *Energy Storage Mater.* **2019**, *18*, 92.
[180] F. Wang, L. Suo, Y. Liang, C. Yang, F. Han, T. Gao, W. Sun, C. Wang, *Adv. Energy Mater.* **2017**, *7*, 1600922.
[181] F. Wang, Y. Lin, L. Suo, X. Fan, T. Gao, C. Yang, F. Han, Y. Qi, K. Xu, C. Wang, *Energy Environ. Sci.* **2016**, *9*, 3666.
[182] G. Gardner, J. Al-Sharab, N. Danilovic, Y. B. Go, K. Ayers, M. Greenblatt, G. C. Dismukes, *Energy Environ. Sci.* **2016**, *9*, 184.
[183] D. J. Hand, K. Yu, *Int. Stat. Rev.* **2001**, *69*, 385.
[184] C. J. C. Burges, *Data mining and knowledge discovery* **1998**, *2*, 121.
[185] W. S. Noble, *Nat. Biotechnol.* **2006**, *24*, 1565.
[186] S. R. Safavian, D. Landgrebe, *IEEE Trans. Syst., Man, Cybernet.* **1991**, *21*, 660.
[187] M. Belgiu, L. Dragut, *ISPRS J. Photogramm Remote Sens.* **2016**, *114*, 24.
[188] H. Aytug, C. Saydam, *Eur. J. Oper. Res.* **2002**, *141*, 480.
[189] J. Zou, Y. Han, S.-S. So, in *Artificial neural networks: methods and applications*, Humana Press, Totowa, NJ **2009**, pp. 14–22.
[190] A. Cully, J. Clune, D. Tarapore, J.-B. Mouret, *Nature* **2015**, *521*, 503.
[191] K. T. Butler, D. W. Davies, H. Cartwright, O. Isayev, A. Walsh, *Nature* **2018**, *559*, 547.
[192] Y. Zhang, C. Ling, *Npj Comp. Mater.* **2018**, *4*, 25.
[193] V. L. Deringer, M. A. Caro, G. Csányi, *Adv. Mater.* **2019**, *31*, 1902765.
[194] J. Wei, X. Chu, X.-Y. Sun, K. Xu, H.-X. Deng, J. Chen, Z. Wei, M. Lei, *InfoMat* **2019**, *1*, 338.
[195] J. Schmidt, M. R. G. Marques, S. Botti, M. A. L. Marques, *npj Comput. Mater.* **2019**, *5*, 83.
[196] C. Gao, X. Min, M. Fang, T. Tao, X. Zheng, Y. Liu, X. Wu, Z. Huang, *Adv. Funct. Mater.* **2022**, *32*, 2108044.
[197] X. Mi, L. Tian, A. Tang, J. Kang, P. Peng, J. She, H. Wang, X. Chen, F. Pan, *Comput. Mater. Sci.* **2022**, *201*, 110881.
[198] C. Sutton, M. Boley, L. M. Ghiringhelli, M. Rupp, J. Vreeken, M. Scheffler, *Nat. Commun.* **2020**, *11*, 4428.
[199] S. Zeng, Y. Zhao, G. Li, R. Wang, X. Wang, J. Ni, *NPJ Comput. Mater.* **2019**, *5*, 84.
[200] D. T. Fullwood, S. R. Niezgoda, B. L. Adams, S. R. Kalidindi, *Prog. Mater. Sci.* **2010**, *55*, 477.
[201] J. Tian, R. Xu, Y. Wang, Z. Chen, *Energy* **2021**, *221*, 119682.
[202] R. Suarez-Hernandez, G. Ramos-Sánchez, M. A. Oliver-Tolentino, I. González, *Electrochim. Acta* **2021**, *397*, 139240.
[203] Z. Fei, Z. Zhang, F. Yang, K.-L. Tsui, L. Li, *J. Energy Storage* **2022**, *52*, 104936.
[204] L. Ma, C. Hu, F. Cheng, *J. Energy Storage* **2021**, *37*, 102440.
[205] S. Müller, C. Sauter, R. Shunmugasundaram, N. Wenzler, V. De Andrade, F. De Carlo, E. Konukoglu, V. Wood, *Nat. Commun.* **2021**, *12*, 6205.
[206] J.-J. Li, Y. Dai, J.-C. Zheng, *Front. Phys.* **2022**, *17*, 13503.
[207] S. Khaleghi, D. Karimi, S. H. Beheshti, Md. S. Hosen, H. Behi, M. Berecibar, J. Van Mierlo, *Appl. Energy* **2021**, *282*, 116159.
[208] M. Faraji Niri, G. Apachitei, M. Lain, M. Copley, J. Marco, *Energy Technol.* **2022**, *10*, 2200893.
[209] J. Zhu, Q. Zhang, L. Mereacre, X. Wang, B. Jiang, H. Dai, X. Wei, M. Knapp, H. Ehrenberg, *Energy Technol.* **2022**, *10*, 2200437.
[210] X. Tang, K. Liu, K. Li, W. D. Widanage, E. Kendrick, F. Gao, *Patterns* **2021**, *2*, 100302.
[211] C. Wang, K. Aoyagi, P. Wisesa, T. Mueller, *Chem. Mater.* **2020**, *32*, 3741.
[212] Z. Fei, Z. Zhang, F. Yang, K.-L. Tsui, *J. Energy Storage* **2023**, *62*, 106903.
[213] K. Ishida, N. Tanibata, H. Takeda, M. Nakayama, T. Teranishi, N. Watanabe, *Phys. Status Solidi* **2022**, *259*, 2100526.
[214] A. Tsuchimoto, M. Okubo, A. Yamada, *Electrochemistry* **2023**, *91*, 037007.
[215] E. Galiounas, T. G. Tranter, R. E. Owen, J. B. Robinson, P. R. Shearing, D. J. L. Brett, *Energy and AI* **2022**, *10*, 100188.
[216] T. Fu, D. Lu, Z. Yao, Y. Li, C. Luo, T. Yang, S. Liu, Y. Chen, Q. Guo, C. Zheng, *J. Mater. Chem. A* **2023**, *11*, 13889.
[217] L. Massimiliano, University of Rome "La Sapienza", **2019**.
[218] C.-A. Lin, S.-K. Lin, *JOM* **2022**, *74*, 4654.
[219] M. Akhilash, P. S. Salini, B. John, S. Sujatha, T. D. Mercy, *Chem. Rec.* **2023**, *23*, e202300132.
[220] A. Dineva, B. Csomós, S. Kocsis Sz, I. Vajda, *J. Energy Storage* **2021**, *36*, 102351.
[221] H. Adenusi, G. A. Chass, S. Passerini, K. V. Tian, G. Chen, *Adv. Energy Mater.* **2023**, *13*, 2203307.
[222] X. Wang, S. Li, W. Zhang, D. Wang, Z. Shen, J. Zheng, H. L. Zhuang, Y. He, Y. Lu, *Nano Energy* **2021**, *89*, 106353.
[223] J. Liu, H. Yuan, X.-B. Cheng, W.-J. Chen, M.-M. Titirici, J.-Q. Huang, T.-Q. Yuan, Q. Zhang, *Mater. Today Nano* **2019**, *8*, 100049.
[224] R. S. Negi, M. T. Elm, *Scientific Data* **2022**, *9*, 127.
[225] X. Gao, X. Liu, R. He, M. Wang, W. Xie, N. P. Brandon, B. Wu, H. Ling, S. Yang, *Energy Storage Mater.* **2021**, *36*, 435.
[226] D. Wu, X. Li, X. Liu, J. Yi, P. Acevedo-Peña, E. Reguera, K. Zhu, D. Bin, N. Melzack, R. Wills, *J. Phys.: Energy* **2022**, *4*, 041501.
[227] Z. Hou, M. Dong, Y. Xiong, X. Zhang, Y. Zhu, Y. Qian, *Adv. Energy Mater.* **2020**, *10*, 1903665.
[228] H. Zhang, X. Liu, H. Li, I. Hasa, S. Passerini, *Angew. Chem., Int. Ed.* **2021**, *60*, 598.
[229] Y. Liang, Y. Yao, *Nat. Rev. Mater.* **2023**, *8*, 109.
[230] Z. Liu, Y. Huang, Y. Huang, Q. Yang, X. Li, Z. Huang, C. Zhi, *Chem. Soc. Rev.* **2020**, *49*, 180.
[231] H. Ao, Y. Zhao, J. Zhou, W. Cai, X. Zhang, Y. Zhu, Y. Qian, *J. Mater. Chem. A* **2019**, *7*, 18708.
[232] N. Patil, A. Mavrandonakis, C. Jérôme, C. Detrembleur, J. Palma, R. Marcilla, *ACS Appl. Energy Mater.* **2019**, *2*, 3035.
[233] D. Chao, S.-Z. Qiao, *Joule* **2020**, *4*, 1846.
[234] R. Demir-Cakan, M. R. Palacin, L. Croguennec, *J. Mater. Chem. A* **2019**, *7*, 20519.
[235] J. Han, A. Mariani, S. Passerini, A. Varzi, *Energy Environ. Sci.* **2023**, *16*, 1480.

[236] D. Pahari, S. Puravankara, *ACS Sustain. Chem. Eng.* **2020**, *8*, 10613.
[237] M. Akhilash, P. S. Salini, B. John, T. D. Mercy, *J. Alloys Compd.* **2021**, *869*, 159239.
[238] B. Huang, Y.-I. Jang, Y.-M. Chiang, D. R. Sadoway, *J. Appl. Electrochem.* **1998**, *28*, 1365.
[239] S. Posada-Pérez, G. Hautier, G.-M. Rignanese, *J. Phys. Chem. C* **2021**, *126*, 110.
[240] X. Wu, J. Ma, J. Wang, X. Zhang, G. Zhou, Z. Liang, *Global Challenges* **2022**, *6*, 2200067.
[241] T. G. T. A. Bandara, J. C. Viera, M. González, *Renew. Sustain. Energy Rev.* **2022**, *162*, 112338.
[242] A. Dave, J. Mitchell, S. Burke, H. Lin, J. Whitacre, V. Viswanathan, *Nat. Commun.* **2022**, *13*, 5454.
[243] J. Entwistle, R. Ge, K. Pardikar, R. Smith, D. Cumming, *Renew. Sustain. Energy Rev.* **2022**, *166*, 112624.
[244] A. Dave, J. Mitchell, K. Kandasamy, H. Wang, S. Burke, B. Paria, B. Póczos, J. Whitacre, V. Viswanathan, *Cell Rep. Phys. Sci.* **2020**, *1*, 100264.
[245] G. A. Giffin, *Nat. Commun.* **2022**, *13*, 5250.
[246] W. Gao, N. Krins, C. Laberty-Robert, H. Perrot, O. Sel, *J. Phys. Chem. C* **2021**, *125*, 3859.
[247] A. Lakshmi-Narayana, K. Sivajee-Ganesh, M. Dhananjaya, A. Narayan-Banerjee, C. M. Julien, S.-W. Joo, *Batteries* **2022**, *8*, 149.
[248] L. Xue, Q. Zhang, Y. Huang, H. Zhu, L. Xu, S. Guo, X. Zhu, H. Liu, Y. Huang, J. Huang, L. Lu, S. Zhang, L. Gu, Q. Liu, J. Zhu, H. Xia, *Adv. Mater.* **2022**, *34*, 2108541.

Hailing Ma is currently pursuing a Ph.D. in Mechanical Engineering at the University of New South Wales, Canberra campus. Previously, he worked as a Research Assistant at the Hoffmann Institute of Advanced Materials. His research interests lie in catalysts for energy materials and environmental applications, with a special focus on the development and application of computational-based techniques used in conjunction with experiments for probing complex material properties. His work mainly emphasizes those properties significant in catalysis and energy technologies.

Fei Wang received his Master degree in materials science and engineering from Shenzhen University in 2021. He was working as a research assistant in Prof. Hanlin Hu's group, at Hoffmann Institute of Advanced Materials, Shenzhen Polytechnic. He is currently a joint Ph.D. student of Wuhan University of Technology & Hoffmann Institute of Advanced Materials. His research interests include new energy lithium-ion batteries and photovoltaic devices.

Tong Yao, an Industrialization Engineer (Assistant Researcher) at the Hoffman Institute of Advanced Materials. He graduated with a bachelor's degree from Beijing University of Chemical Technology and obtained his Ph.D. from the Song Mo research group at the Materials College of Loughborough University, UK, in 2016. He has published over ten academic papers, including five as the first author or corresponding author, one academic monograph, and holds two corporate patents. After returning to China, he worked at Shenzhen Wotema Battery and a foreign-funded carbon material unicorn company, serving in roles such as Assistant to the President, Assistant Quality Director, and Technical Manager. His primary research focus is on the application of graphene and carbon nanotubes in the field of lithium batteries.

Hongxu Wang is a Lecturer working in the School of Engineering and Technology at the University of New South Wales (UNSW) Canberra. His research interests center on composite materials, impact dynamics, 3D printed materials, energy absorption structures, etc. He has published over 50 journal articles and received more than 1300 citations as of December 2023.

Hanlin Hu obtained his Ph.D. degree in Department of Materials Science and Engineering at King Abdullah University of Science & Technology in Saudi Arabia in 2017. He carried out his post-doctorate research at the Hong Kong Polytechnic University. He is currently the director of SPRAY-ON PEROVSKITE PHOTOVOLTAIC R&D CENTER at Shenzhen Polytechnic University. He has built Synchrotron and Printable Electronic Devices Lab at HIAM equipped with in-house GIWAXS/GISAXS. He has published 120+ papers with an H index of 31. His research focuses on printing thin film solar cells, transistors, energy storage materials, and the synchrotron-based phase-transition study.